NASA TECHNICAL NOTE

NASA TN D-4910

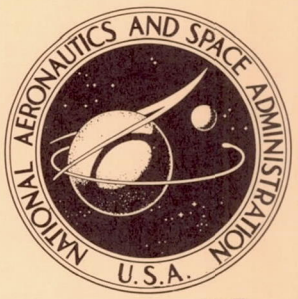

NASA TN D-4910

HIGH-FIELD ELECTROMAGNETS AT NASA LEWIS RESEARCH CENTER

by James C. Laurence

Lewis Research Center

Cleveland, Ohio

NATIONAL AERONAUTICS AND SPACE ADMINISTRATION • WASHINGTON, D. C. • NOVEMBER 1968

NASA TN D-4910

HIGH-FIELD ELECTROMAGNETS AT NASA LEWIS RESEARCH CENTER

By James C. Laurence

APPENDIX A: HOMOPOLAR GENERATOR CONTROLLER

By Erwin H. Meyn

APPENDIX B: ELECTRONIC RAMP-AND-HOLD FUNCTION GENERATOR AS CHARGING CONTROL FOR ELECTROMAGNET

By Russell J. Jirberg

Lewis Research Center
Cleveland, Ohio

NATIONAL AERONAUTICS AND SPACE ADMINISTRATION

For sale by the Clearinghouse for Federal Scientific and Technical Information
Springfield, Virginia 22151 – CFSTI price $3.00

ABSTRACT

The NASA Lewis Research Center has acquired several high-field magnets with field strengths in the range of 3 to 20 teslas. These include conventional, water-cooled copper magnets and cryogenically cooled (superconductive and nonsuperconductive) magnets. The design, construction details, and performance of these magnets are described in this report. The devices which are used to power and control the magnets are likewise described.

HIGH-FIELD ELECTROMAGNETS AT NASA LEWIS RESEARCH CENTER

by James C. Laurence

Lewis Research Center

SUMMARY

Over the past ten years, in response to research requirements, a program has been carried out at NASA Lewis Research Center to develop high-field electromagnets. Early in the program, water-cooled copper solenoids in the 10-tesla range were developed. These magnets were limited in their high-field capabilities by the power available to supply them. Subsequently, neon-cooled aluminum coils were designed, and two large electromagnets in the 15- to 20-tesla range were developed.

In the early 1960's the advent of superconductors with high field capability resulted in the construction of large superconductive magnets with field strengths up to 14 teslas and large working volumes (15 cm diam).

The design, construction, and testing of these magnets are described in this report. The devices which are used to power and control the magnets are also described.

INTRODUCTION

The Lewis Research Center has primary NASA responsibility for research on advanced concepts of power generation and propulsion. Some of these concepts require intense, large-volume, magnetic fields, generated by lightweight equipment with low power consumption. Electric propulsion, magnetohydrodynamic power generation, thermonuclear power and propulsion, space radiation shielding, and reentry of spacecraft into the Earth's atmosphere are some of the concepts for which such magnetic fields may be required. In addition, the development of intense magnetic fields is of importance for studies in a variety of disciplines, such as elementary particle physics (accelerators, bubble chambers), solid-state physics, and plasma physics.

In 1957 (the beginning of magnet research and development at the Lewis Research Center) most large, high-field electromagnets were constructed of copper coils cooled by water (refs. 1 and 2). At that time the Massachusetts Institute of Technology had magnets, designed by Bitter (ref. 2), in the 10-tesla range which used several megawatts of

power at 170 to 180 volts. Because of this voltage, the Bitter design required very good interturn insulation and deionized water for the coolant. Both of these requirements are expensive and difficult to provide. For example, for the large test volumes desired, deionized water would be difficult to produce and store in sufficient quantity. Hence, a large heat exchanger would be needed to transfer the heat generated in the coils to a reservoir of untreated water. This type of system uses pumps, filters, and associated equipment which can become expensive.

When the program to provide large-volume, intense magnetic fields was initiated at the Lewis Research Center, many different means of producing these fields were investigated. To reduce structural problems and simplify magnet construction and operation, it was decided to use low-impedance, high-current design. This design criterion was applied first to the copper water-cooled coils, and later to the aluminum cryogenically cooled coils. The magnets and power sources which resulted from this program are described in this report.

A homopolar generator controller and an electronic ramp-and-hold function generator for charging control of electromagnets are described by Erwin H. Meyn and Russell J. Jirberg in appendixes A and B, respectively.

Major contributions to the design of the magnets and control systems described in this report were made by the following persons: Paul R. Aron, Gerald V. Brown, Edmund E. Callaghan, Willard D. Coles, John C. Fakan, Wayne R. Hudson, Russell J. Jirberg, and Erwin H. Meyn.

POWER SUPPLIES

Homopolar Generator

A large homopolar generator (ref. 3) was selected as the best power source for the low-impedance electromagnets to be constructed. These windings are powered by a separate motor generator set with a controllable output. The charges induced on the rotating cylinder are collected by two flowing streams of a sodium-potassium alloy (NaK). These charges are transferred to bus bars which carry the current to the load. Figure 1 is a photograph of the homopolar installation. The motor switch gear, the exciter set, the generator, the NaK pumps, and the speed increaser are shown in this photograph.

The operating range of the generator and its associated equipment and a response curve are shown in figure 2 up to the 1-minute limit. The continuous rating, however, is 60 000 amperes at 1.8 megawatts. The upper current limit is determined by the current capacity of the steel rotor so as to avoid overheating, which would destroy the insulation on the rotor.

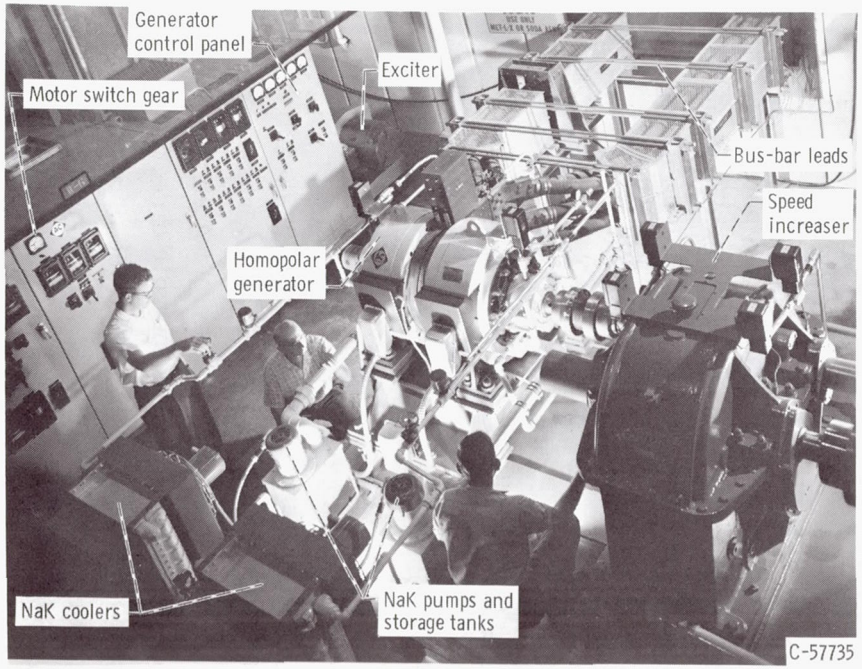

Figure 1. - Homopolar generator installation. (Drive motor is off picture to right.)

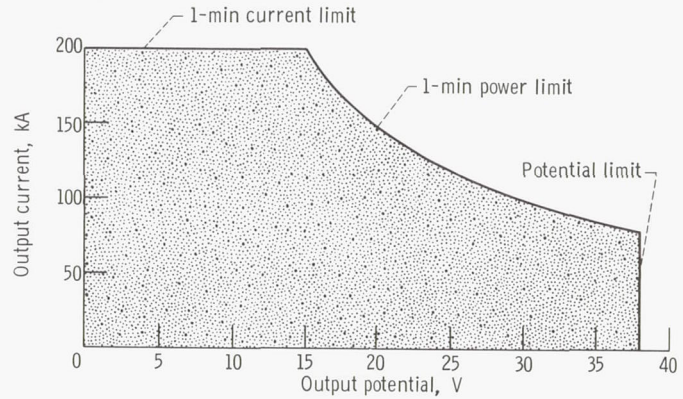

(a) Range of operation.

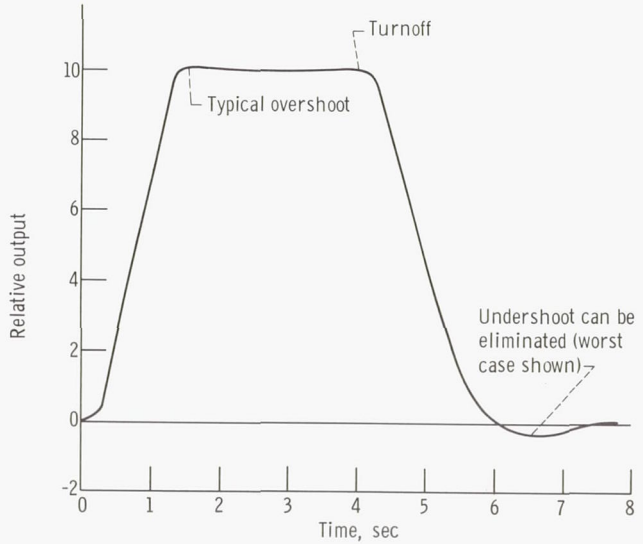

(b) Typical response curve.

Figure 2. - Operational characteristics and typical response curve of the homopolar generator.

The output potential (fig. 2(a)) of the generator is a function of the rotational speed and the field power. The constant rotational speed limits the maximum voltage to 38 volts because of the generator field windings, the associated iron saturation, and the maximum output of the exciter. The electromotive force of the homopolar generator is controlled through the control of the exciter set. The machine can be operated in two modes. Since the internal resistance of the generator is only a few microhms, one mode of operation provides a constant-voltage or zero-impedance characteristic whereby the system current is determined by the load resistance. In the other mode, the current regulation is independent of load resistance and thus constitutes a constant-current system.

Since the time constant of the generator circuit is large (about 2.5 sec) compared with the desired current rise time in magnet applications, the automatic control circuit uses a forcing technique to raise the output to 90 percent of the preselected value (fig. 2(b)) in about 1 second. By use of proper circuitry (see appendix A) this driving voltage can be reversed in polarity and the voltage can be used to drive the current to zero very quickly. This field-forcing feature is most valuable when the generator is used, as it is at Lewis, to power an electromagnet of high inductance, long time constant, high energy storage, and limited capacity of cryogenic coolant.

An electronic ramp-and-hold control for the homopolar generator has been designed and used successfully to control the rate of increase or decrease of the current (appendix B).

This generator and control system has proved to be an excellent magnet power supply. The ripple in the supply voltage is for practical purposes nonexistent (<1 mV at full rated current). The maintenance problems have been concerned primarily with supplying the NaK system with a continuous dry cover gas, such as nitrogen or argon, and limiting the very high current runs so that the rotor insulation is not damaged by overheating.

Transformer-Rectifier System

In addition to the homopolar generator a transformer-rectifier power supply is used to power some of the electromagnets. This system is a three-phase, full-wave rectifier supplied from variable-voltage transformers.

In figure 3, which shows one phase of the rectifier power supply, the 440-volt, 60-hertz input is regulated to compensate for line voltage variations. This voltage is then applied to a pair of variable transformers. The movable contact wipers of this variable set of transformers (T-1 and T-2) travel in opposite directions. When both wipers tap equal potential points, zero voltage is supplied to the primary of transformer T-3; its secondary has no voltage drop across it. The voltage drop across the primary of transformer T-4 is then 440 volts. However, when the voltage taps of T-1 and T-2 are at op-

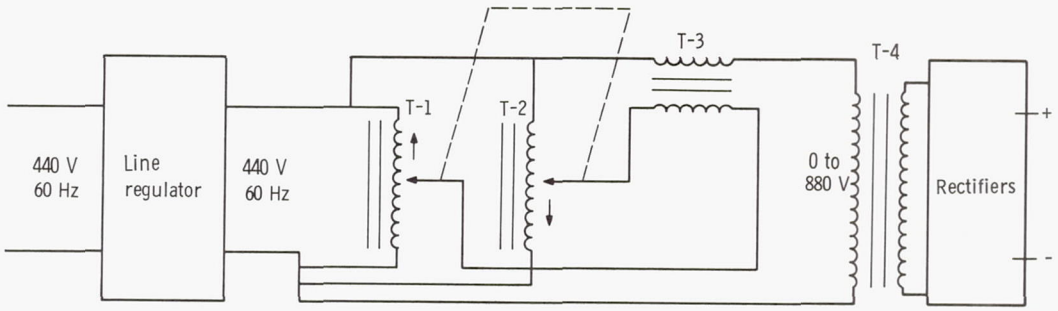

Figure 3. - Schematic diagram of rectifier power supply.

posite ends of the tapped windings, 440 volts will be supplied to the primary of T-3. The one-to-one winding ratio of T-3 will, therefore, produce 440 volts across the secondary of T-3. If the phase of this voltage, which is in series with the 440-volt line, is subtractive, then the voltages will cancel and apply zero volts to T-4. Conversely, the opposite extremes of T-1 and T-2 will yield 440 volts of the opposite polarity across the secondary of T-3, which is additive, and T-4 will be energized with 880 volts on its primary.

This variation, to 880 volts, presented to the rectifiers connected in a three-phase bridge circuit from the three-phase, step-down rectifier-transformer controls the output of the supply from 0 to 45 volts dc. This power source is capable of supplying 15 000 amperes continuously or 30 000 amperes for 2 minutes.

Flux Pump

For superconducting magnets, large persistent currents are built up in small steps by flux pumping. The flux pumping can be done mechanically, by a rotating shaft which provides the energy to be stored, or electrically.

The flux pump developed for the Lewis Research Center operates entirely electrically (ref. 4). The low-voltage, low-current ac input to the cryogenic part of the circuit is carried by small conductors which minimize the heat leak into the Dewar.

The flux-pump circuit, shown in figure 4, operates very much like a full-wave rectifier, with special superconducting switches replacing the rectifiers. These superconducting switches resist the flow of the current in the reverse direction only if they are driven normal by the application of a field or a thermal pulse. In this case the switches have zero resistance in the forward direction and normal-state resistance in the reverse direction. The current is supplied through a step-down transformer wound with a superconductor to two saturable reactors and the superconducting switches. The switches are alternately opened and closed by the voltage swings of the superconducting transformer.

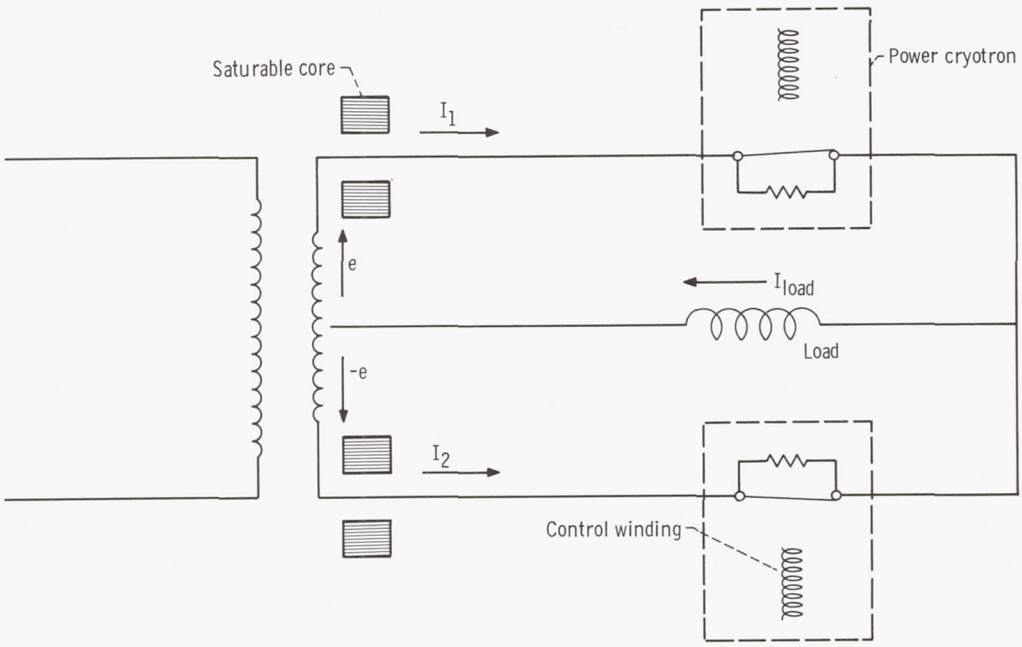

Figure 4. - Schematic diagram of flux-pump circuit.

Therefore, the ac current through the magnet coil (the load) builds up in a series of steps. By proper phasing of the superconducting switches, the energy can also be removed from the magnet and dissipated in the external circuit.

The flux pump in use furnishes 1750 amperes maximum of charging current in a time interval of 60 seconds to a load of 2×10^{-3} henry.

NORMAL CONDUCTOR MAGNETS

The unique feature of the homopolar generator - a very low ratio of output voltage to current - leads to certain advantages in designing the magnets. The following are three of these advantages:

(1) The magnet windings can be made in large cross section of high-purity material to take advantage of the very heavy currents that can be drawn from the machine. These conductors are inherently stronger because of their size and may be nearly self-supporting in the fields produced.

(2) Since the potential difference between turns of a magnet designed according to this concept is small (of the order of 1 or 2 V) no special high-voltage insulation or water treatment is necessary. The cooling water can be drawn from the mains and disposed of

in the sewer. In addition, there are no hazards because of high voltage.

(3) Cryogenic cooling of the conductors, which reduces their resistance by a factor of 1000 or more, can be used in the design and can be adapted to the low output impedance of the generator.

Water-Cooled Copper Solenoids

Two water-cooled magnets have been designed and built to operate from the homopolar generator (ref. 3). In each of these a helix was formed from a solid billet of commercial-grade copper of circular cross section. The billet was bored to a convenient diameter smaller than the desired final inside diameter and a length of steel pipe was fitted into the hole. By cutting a deep spiral cut nearly to the pipe (which was added for stability and support during the machining) and then removing the pipe and boring the inside diameter to the final value a helix was formed. Radially directed insulating spacers, 0.063 centimeter thick, 1 centimeter wide at the outer radius of the helix, and 0.1 centimeter wide at the inner radius, were placed at 15° increments between turns of the helix (fig. 5). The helix was then collapsed onto the spacers to form the magnet core. This core was attached to large bus connectors at the ends and encased in a housing which provides for coolant passages concentric with the magnet bore at the inner and outer periph-

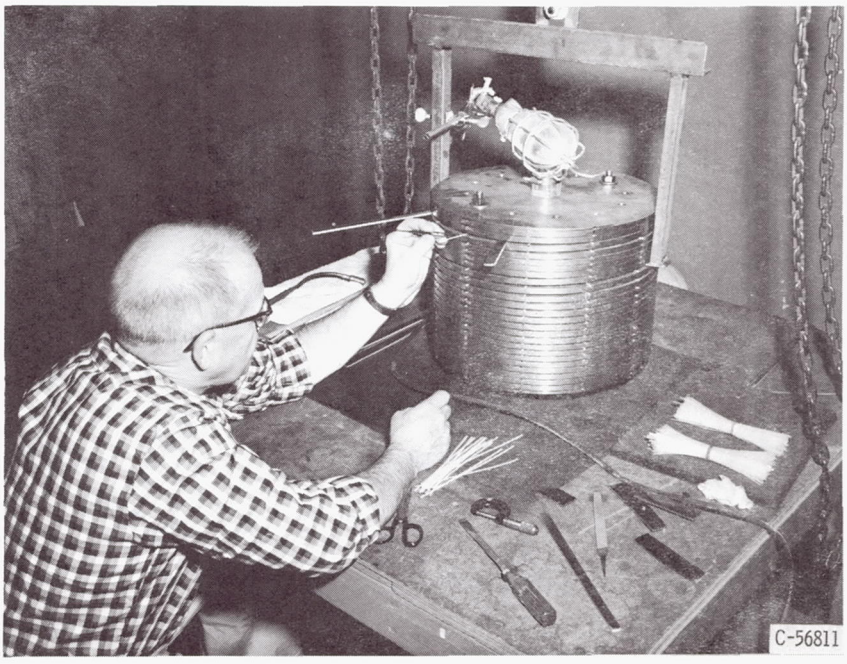

Figure 5. - Assembly of spacers in core of 11-tesla water-cooled electromagnet.

TABLE I. - SPECIFICATIONS OF WATER-COOLED MAGNETS

Specification	Magnet	
	5-cm bore	10-cm bore
Number of turns	24	20
Thickness of turns, cm	0.95	2.032
Spacing between turns, cm	0.064	0.102
Packing fraction	0.94	0.97
Inner diameter of coil, cm	5	10
Outer diameter of coil, cm	40	50
Ratio of outer to inner diameter of coil	8.00	5.0
Ratio of length to inner diameter of coil	4.85	4.2
Inner diameter of liquid-helium Dewar, cm	1.6	6.0
Inner diameter of magnet core at room temperature, cm	4.6	8.9
Maximum magnetic field, T	11.0	8.85
Current, kA	90	150
Total voltage, V	18	13.8
Voltage between turns, V	0.6	0.7
Cooling-water flow rate at 4×10^5 N/m^2 pressure, kg/sec	18.2	38.4
Cooling-water temperature rise, ^oC	22	13
Ratio of magnetic field to current, T/A	1.15×10^{-4}	0.59×10^{-4}
Stored energy per unit volume, J/cm^3	47.9	31.00

eries. The dimensions and operational characteristics of these two magnets are given in table I.

The cooling water flows in at the bottom center of the magnet and then radially outward between the turns to the periphery where it is collected and discharged (fig. 6). The water is drawn directly from the mains at normal city water pressure and, because of the low potential drop ($\leq$1 V) between turns, requires no special treatment. The water flow rate is from 10 to 40 kilograms per second.

Some of the other noteworthy features of these water-cooled magnets are the high packing fractions (ratio of conductor volume to the total volume of the coils) of 0.94 and 0.97, the small temperature rise of the cooling water, the distribution of the current which is inversely proportional to radius (most current where the magnet produces the most field), and the amounts of energy stored per unit volume (47.9 and 31.0 J/cm^3). The massive size of the conductors, 2.0-centimeter-thick by 50-centimeter-diameter copper plates, make the magnets self-supporting with no volume sacrificed to non-current-carrying structures.

Of importance to the experimenter is the volume in the field available for apparatus. Of particular interest is test volume inside a controlled-temperature Dewar. For experiments these magnets and associated Dewars have clear working diameters of 1.6 and

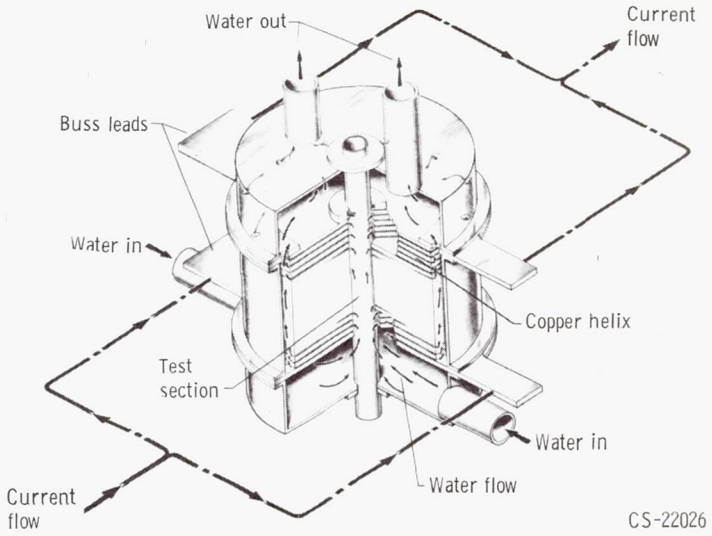

Figure 6. - Flow diagram of 11-tesla water-cooled electromagnet.

6.0 centimeters, respectively, in liquid helium. The cost of each of the magnet coils was less than $6000.

The water-cooled magnet system, including the magnet and homopolar generator, was later reproduced at the magnet laboratory of the NASA Jet Propulsion Laboratory (ref. 5).

Cryogenically Cooled Aluminum Magnets

It is hard to get high current density, structural strength, and low power consumption simultaneously in magnet windings. It is still harder to use the conductor material itself as the structure. The massive turns of the previously described water-cooled magnets were self-supporting, but at much higher densities pure copper is not strong enough to support itself. Some copper alloys (BeCu, ZrCu, etc.) have much higher strength with only moderately increased resistivity. However, still greater gains in strength and much lower resistivity are possible with specialization. Many steels with much higher strength than the copper alloys, are better for structural support. On the other hand some high purity metals cooled to cryogenic temperatures have resistivities of only 1/100 to 1/1000 of that of copper at room temperature. Thus it is very desirable to separate the functions of conduction and stress support. Greater strength and lower power consumption result. These are the principal advantages of cryogenically cooled (nonsuperconductive) electromagnets (refs. 6 to 8).

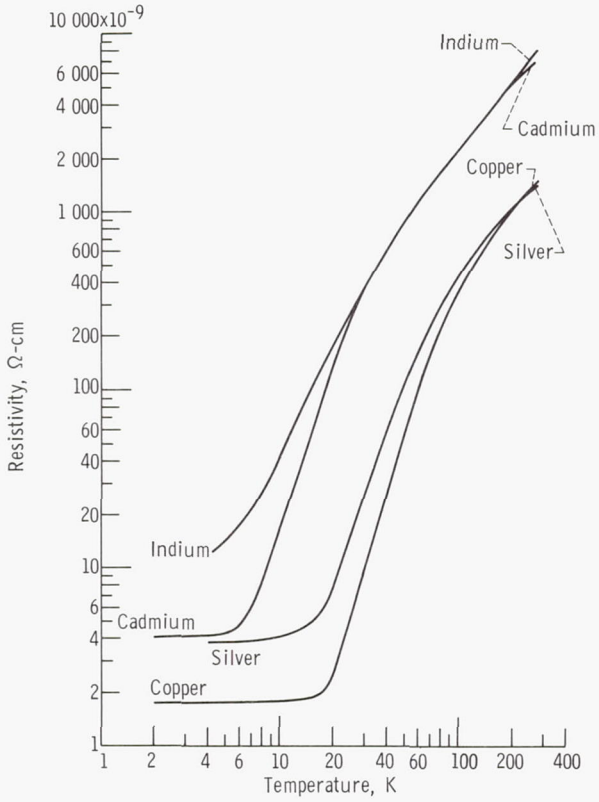

Figure 7. - Resistivity-temperature relation for some pure metals (ref. 9).

The resistivity of commercial-grade (99.9 percent pure) copper at 20 K (the boiling point of liquid hydrogen at atmospheric pressure) is 1/120 of its value at room temperature (293 K), but at 77 K (the boiling point of liquid nitrogen at atmospheric pressure) it is only 1/7 of the resistivity at room temperature. But, as shown in figure 7 (ref. 9), these ratios can be much smaller for very high purity conductors. For example, the National Bureau of Standards has produced samples of copper and aluminum with ratios less than 1/25 000 and, in some instances, have approached 1/40 000. For a 99.9983-percent-pure aluminum (a purity possible without zone refining) these ratios are 1/2000 at 4.2 K and 1/1000 at 20.4 K.

Another significant factor for magnet construction is the magnetoresistivity. The magnetoresistivity of a conductor is that component of its resistivity which is dependent upon the magnetic field in which the conductor is located. In figure 8 the magnetoresistivity of aluminum is plotted as a function of magnetic field for several temperatures of interest. It can be seen that the magnetoresistivity saturates with magnetic field at fields of 1.0 to 5.0 teslas, depending upon the purity of the aluminum and the temperature. The magnetoresistance data for copper, shown in figure 9 (ref. 10), do not exhibit a corres-

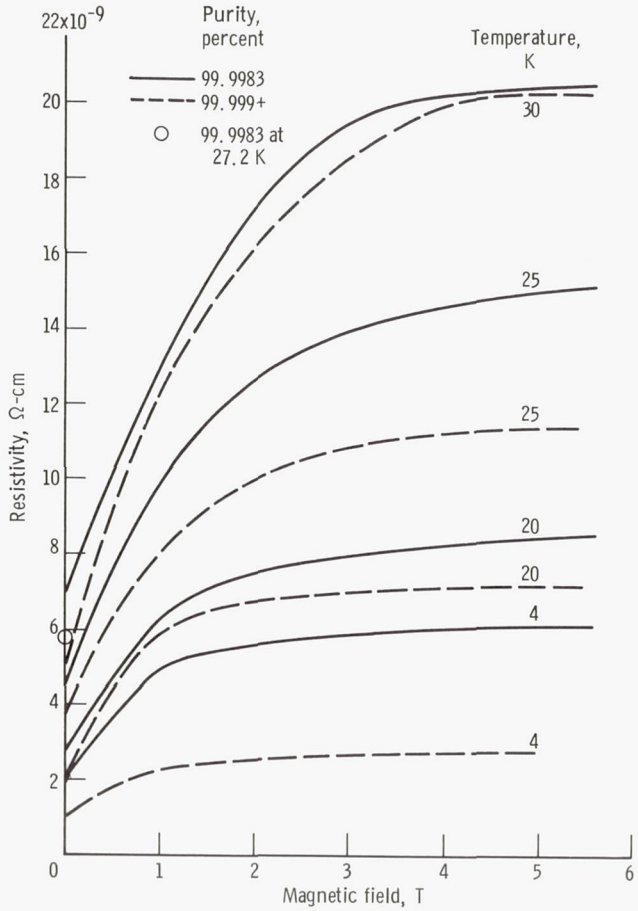

Figure 8. - Magnetoresistivity of aluminum.

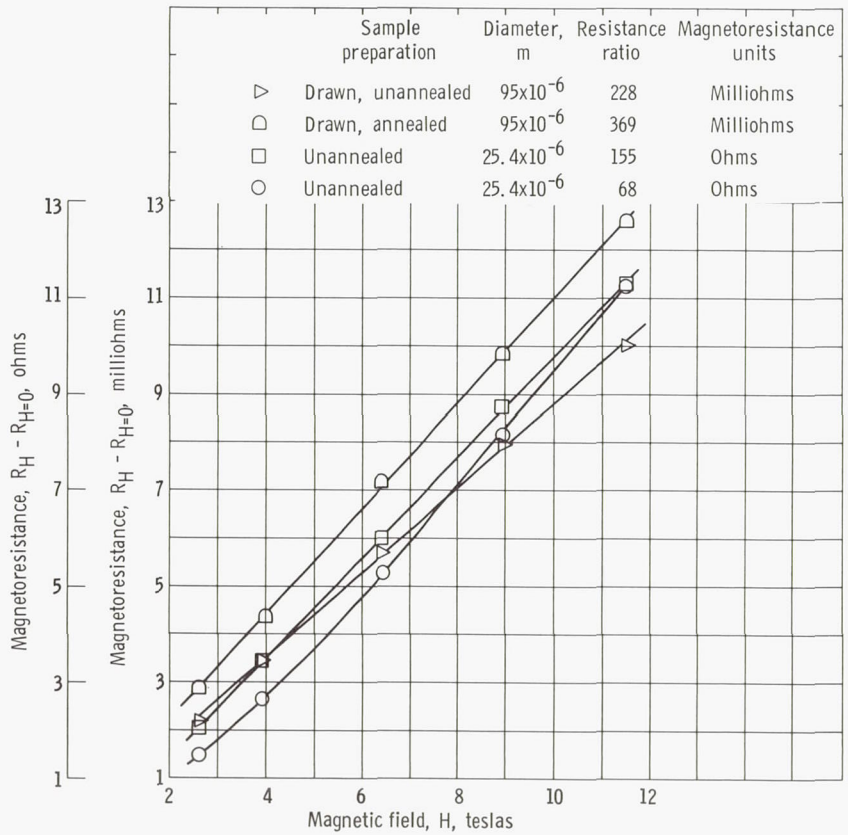

Figure 9. - High-field magnetoresistance of copper.

TABLE II. - SPECIFICATIONS OF CRYOGENICALLY COOLED ALUMINUM MAGNETS

Specification	Magnet	
	11.5-cm bore	30.0-cm bore
Number of coils	8	6
Approximate number of turns per coil	90	75
Packing fraction	0.4	0.4
Inner diameter of coil, cm	13.0	30.5
Outer diameter of coil, cm	94	94
Ratio of outer to inner diameter of coil	7.1	3.1
Ratio of length to inner diameter of coil	4.0	1.3
Inner diameter of liquid-helium Dewar, cm	6.4	23
Inner diameter of magnet core at room temperature, cm	6.4	23
Maximum magnetic field, T	19.9	8.0
Maximum current, kA	30.4	10.0
Total voltage, V	34.3	22.9
Power consumed, MW	1.042	0.229
Ratio of magnetic field to current, T/A	13.1×10^{-4}	8.0×10^{-4}
Total stored energy, MJ	9.4	3.6

ponding saturation. Hence, aluminum becomes a strong candidate for high-field, cryogenically cooled electromagnets. The 99.9983-percent-pure aluminum was chosen as the conductor material for two magnets with inner diameters of 11.5 and 30.0 centimeters, respectively (see table II).

As seen in figure 8, the temperatures which are suitable for cooling an electromagnet are provided quite well by liquid helium at 4.2 K, liquid hydrogen at 20.4 K, and liquid neon at 27.2 K (refs. 11 and 12). Liquid helium is not a good coolant for pool-boiling heat transfer because the latent heat of vaporization ($\approx$20 J/g) is so small. The hazards of liquid hydrogen preclude its use in a populated area such as the Lewis Research Center.

Neon is a rare, inert gas whose only known source is the Earth's atmosphere, where it occurs at a concentration of approximately 18 parts per million. Since neon is inert there are no safety problems except those inherent with any cryogenic liquid. Large-scale production of liquid oxygen for the steel industry during the last decade has made neon available in large supply at a considerable reduction in cost. Even so, at \$30 per standard cubic meter of gas the cost of operating with liquid neon (\$42 per liter) is prohibitive unless the gas is recovered and reliquified for reuse. The capital investment required for the liquid-neon refrigerator and liquifier was one-third (ref. 12) that of a cold-helium gas system large enough to cool the magnets desired. In addition, liquid neon is a very desirable cryogen for use in a boiling heat transfer application because of its large latent heat per unit volume. Hence, liquid neon was chosen as the coolant for the electromagnets.

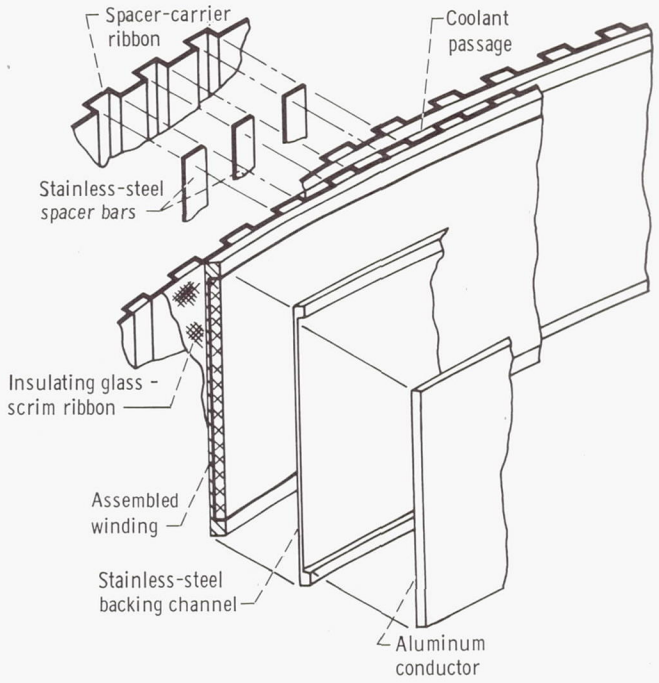

Figure 10. - Construction of coils of cryogenically-cooled aluminum magnet.

The construction of the aluminum coils is shown in figure 10 (ref. 7). Each turn of the magnet consists of a composite structure providing the current path, structural integrity, coolant passages, and insulation. The conductor, processed from 99.9983-percent-pure aluminum, is 5 centimeters wide by 0.2 centimeter thick. It was anodized to produce a uniform coating of aluminum oxide (Al_2O_3) on the surface. This coating serves to insulate the high-purity aluminum from the stainless-steel channel and to improve the boiling heat transfer by providing additional sites for incipient boiling. The channel supports the very soft, annealed aluminum (heat treated at 400° C for 2 hr) on three sides.

The stainless-steel channel in addition to restraining the aluminum provides the hoop strength and much of the turn-to-turn and coil-to-coil bearing surface. Flow channels for the liquid-neon coolant are provided by stainless-steel spacer bars held in place and equally spaced by a thin corrugated carrier ribbon of stainless steel. A glass and epoxy resin cloth provides insulation between turns.

The spacer bars were cemented to the carrier ribbon and these parts were handled as a subassembly. During the coil winding process (fig. 11) a thermosetting bonding agent was applied to all surfaces, except the conductor surface, to be exposed to the coolant.

Additional parts making up the coil assembly are high-purity aluminum center bus rings and outer bus bars, stainless-steel forged outer rings for additional hoop strength,

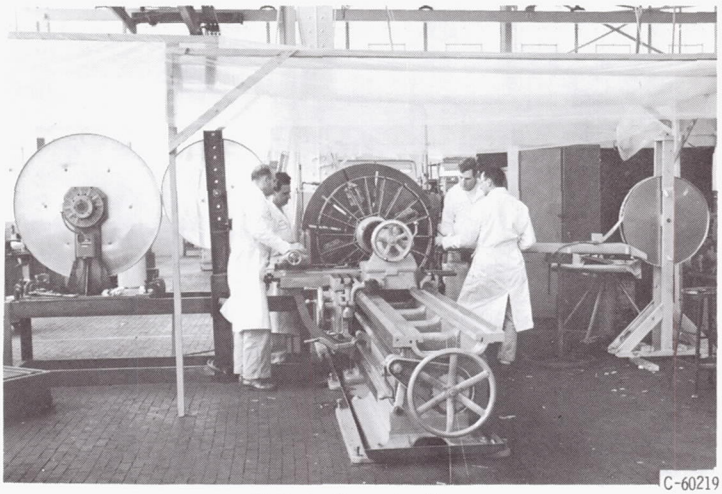
C-60219

(a) Placing the carrier ribbon.


C-60220

(b) Starting the wrap-up.

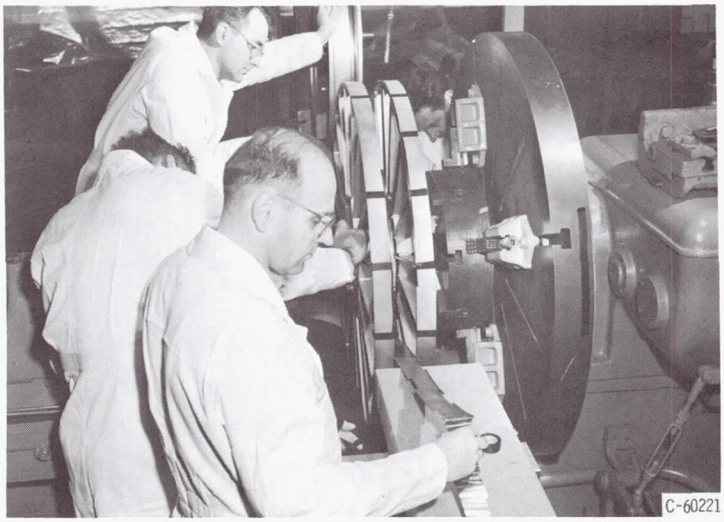
C-60221

(c) Winding the composite conductor, support channel, carrier ribbon, and interturn insulation.

Figure 11. - Winding of aluminum coils.

and glass-epoxy radial coil-spacer and insulation bars. Oven curing of the bonding agent and welding together the center rings of coil pairs completed the winding assembly.

The coils contain approximately 150 meters of the aluminum conductor. The center ring serves two purposes: (1) the conductor is welded to and wound around the ring as a coil form, and (2) the ring transfers the current from one coil to its neighbor to form a magnet pair. The rings are slit vertically and secured with a fiber glass resin insert to interrupt the current in the ring, which otherwise reacts with the changing field to expel the rings.

Two bore sizes of this magnet have been built and operated at the Lewis Research Center. The larger bore is 30 centimeters and the smaller is 11.5 centimeters. The magnet coils are connected in a series - parallel arrangement as shown in figure 12.

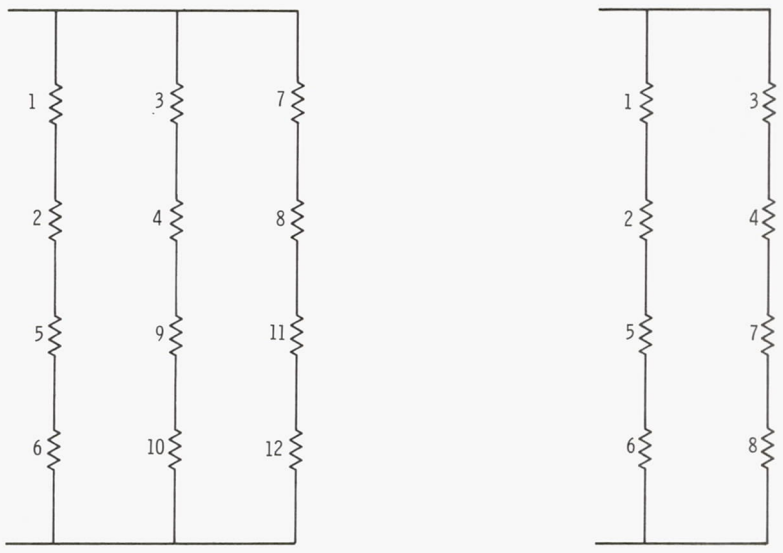

(a) 12-Coil magnet. (b) 8-Coil magnet.

Figure 12. - Electrical connections of aluminum coils in series-parallel circuit.

This arrangement has proved to be efficient in producing the required fields within the voltage limit of the homopolar generator and with a current requirement well within the capability of the generator.

A completed stack of these coils ready to be inserted in the cryostat is shown in figure 13. Clearly shown in this photograph are the bus bars and the supporting structure which prevent their deformation by the interaction of the current and the field. Also shown in the photograph are a series of "arc balls" which are intended to provide a non-destructive path for an arc if a large inductive electromotive force develops because of an accident to a bus bar or other system components.

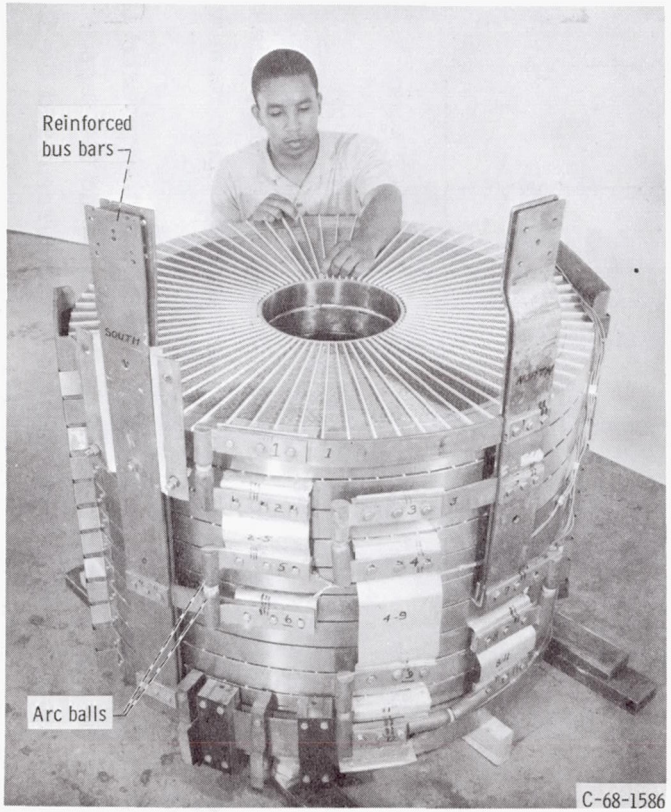

Figure 13. - Complete stack of magnet coils.

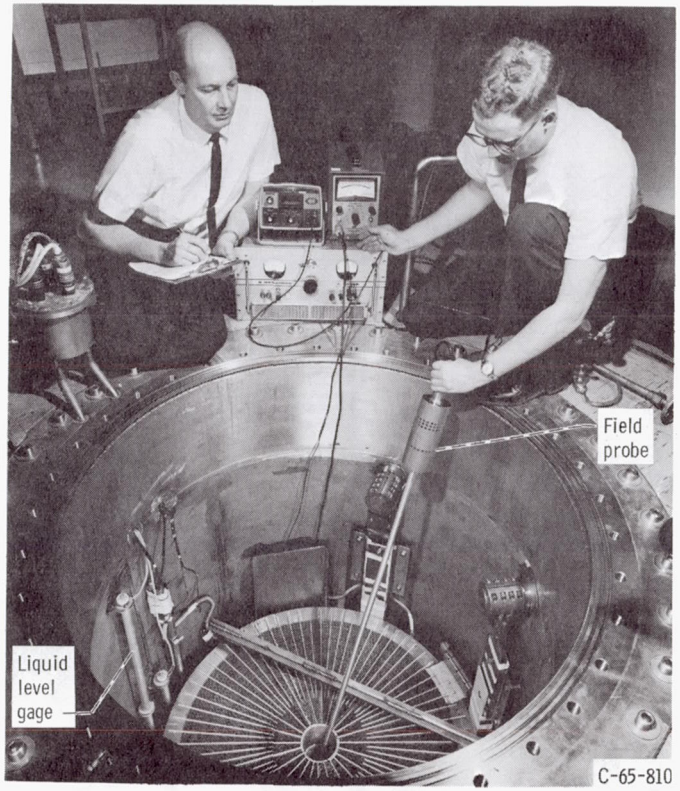

Figure 14. - Magnet coils installed in cryostat.

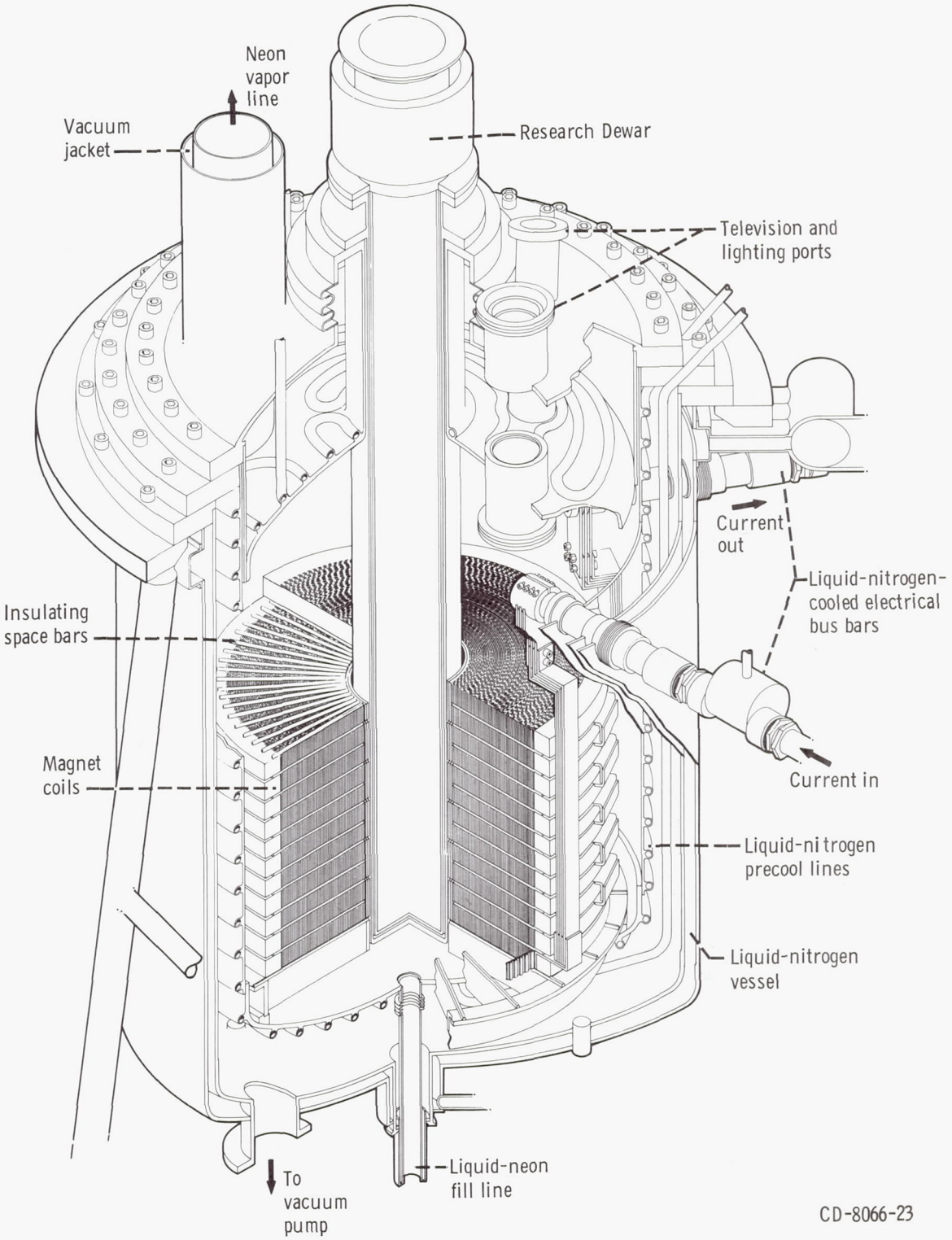

Figure 15. - Liquid-neon-cooled aluminum electromagnet.

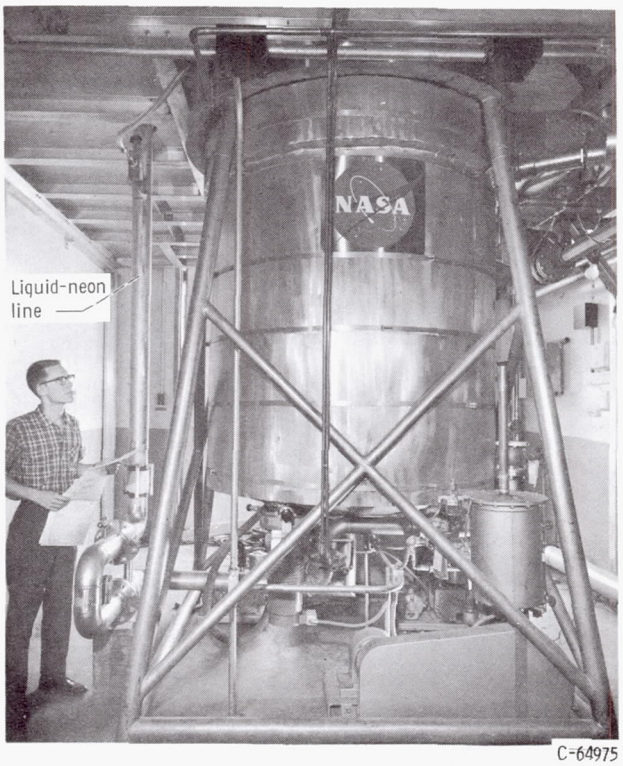

(a) Lower level.

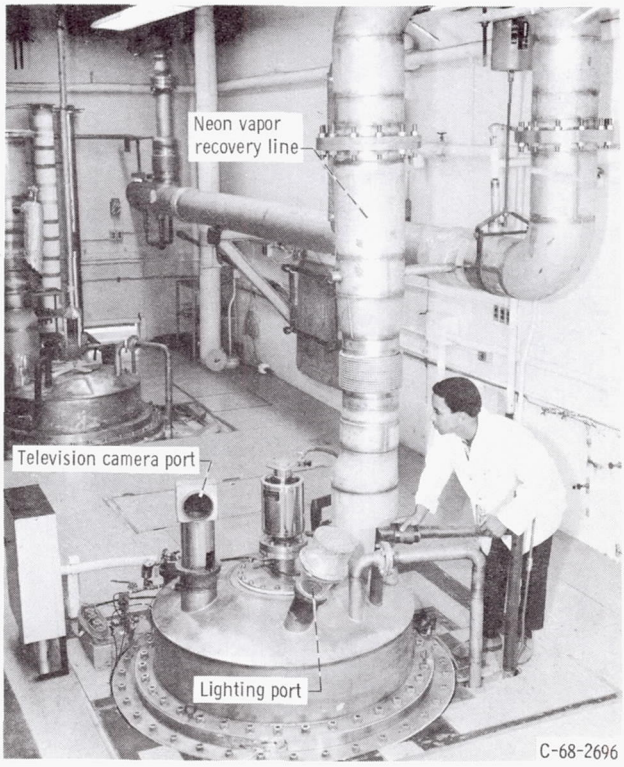

(b) Upper level.

Figure 16. - Liquid-neon-cooled electromagnet containment vessel.

The cryostat, including a complete set of coils, is shown in figure 14. As shown here (11.5-cm-bore coils) the installation is complete and ready for the lid of the cryostat to be put into place and secured. In the picture the capacitance-type liquid level gages are shown mounted on the inner wall of the vessel.

Figure 15 is a schematic drawing of the completed facility, and figure 16 shows photographs of the completed installation. In the schematic (fig. 15) the construction of the cryostat is illustrated with the vacuum jacket, the liquid-nitrogen jacket, and the trace lines for precooling of the magnet vessel and coils. Figure 16(a) shows the vacuum pumps which pump down the vacuum-jacketed lines and vessel. The pipes which carry the liquid neon are shown on the photograph also.

The picture of the top of the cryostat (fig. 16(b)) shows the vapor recovery line which takes the neon gas back to the liquifying plant. Figure 16(b) also shows television and lighting ports and the insert Dewar which provides room-temperature (or any other temperature) access to the magnetic field.

Performance of Cryomagnets

The aluminum cryogenically cooled magnets have been in operation for about 5 years. Some of the data obtained from this program are presented in figures 17 and 18 and table III. The specifications of the two magnets are given in table II and some data from the operation in table III. In figure 17 the power required for the 11.5-centimeter magnet

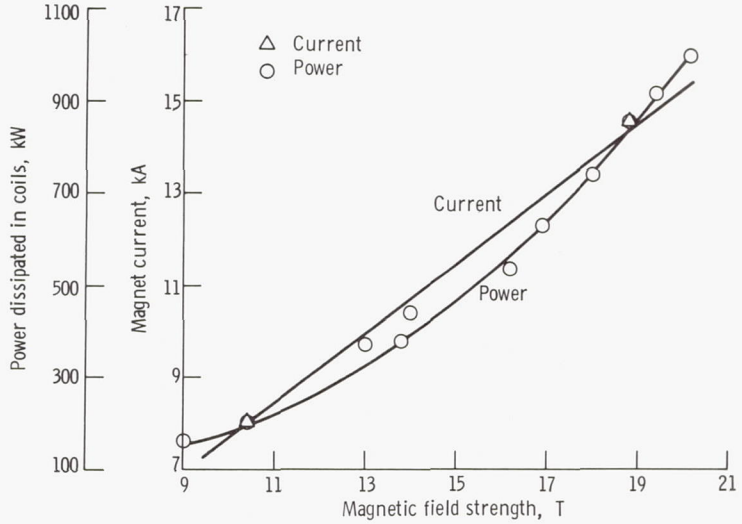

Figure 17. - Performance of 11.5-centimeter-bore cryomagnet. Tesla-ampere ratio, 13.1×10^{-4}.

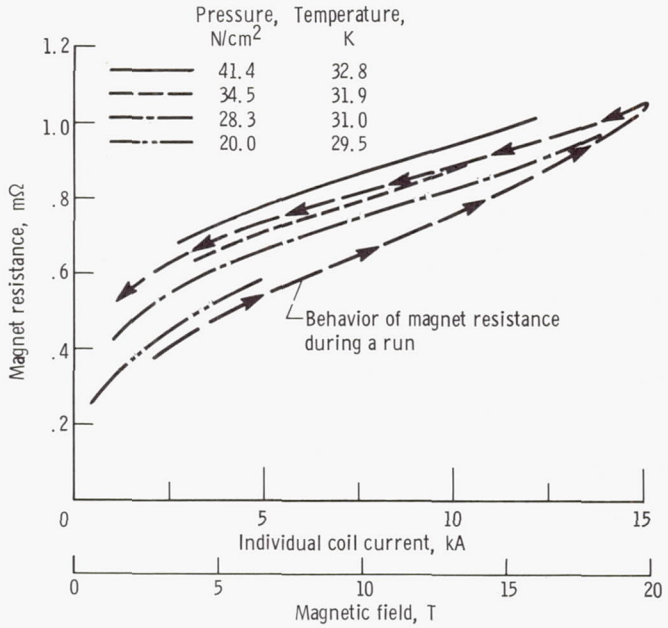

Figure 18. - Resistance of eight 11.5-centimeter-bore coils in series-parallel circuit as function of individual coil current.

TABLE III. - OPERATION OF 11.5-CENTIMETER-BORE CRYOMAGNET

Test	Current, kA	Magnetic field, T	Potential difference across coil, V	Power, kW
1	7.0	9.2	11.6	162
2	9.9	13.0	18.8	372
3	7.9	10.4	12.7	201
4	10.5	13.8	18.0	378
5	12.4	16.2	22.0	545
6	12.9	16.9	24.5	634
7	13.7	18.0	27.0	742
8	14.3	18.8	30.0	858
9	10.7	14.0	20.6	441
10	14.8	19.4	31.0	918
11	15.2	19.9	33.0	1004

is shown over the operating range from 0 to 20.0 teslas. Figure 18 shows the change in resistance of the coils over the same operating range. This change in resistance is caused by the change in magnetoresistance of the aluminum conductor as the field increases and by the heating of the conductor as the current increases during a period of operation.

The operation of the cryogenically cooled magnets is limited by the capacity of the refrigeration system - approximately 80 liters of liquid neon per hour. This limitation can be better expressed as one period of operation per one 24-hour day. The time of a period of operation depends upon the field strength desired. At maximum field (maximum power consumption) the time of operation is about 1 minute total time including time to run up to field, time of operation at desired field strength, and time to shut down. The time is much longer, of course, for lower field ranges. During a typical day's operation, four runs at 4.0 teslas, two at 5.0 teslas, one at 17.7 teslas, and one at 11.0 teslas were achieved.

The power required for the maximum field produced to date is seen from table III to be 1.0 megawatt at 33 volts and 15 200 amperes in each of two parallel sets of coils. These data illustrate two important achievements of the aluminum magnets:

(1) The total power consumed has been substantially reduced (by a factor of 20 or more) from that required for water-cooled magnets of the same field strength and volume of field.

(2) The total current required has been reduced also - by a factor of 3 or 4 - to a range which is much more compatible with the specifications of the homopolar generator. Indeed, the requirements are within the capacity of the rectifier power supply described previously. This second point is only advantageous when compared with the water-cooled magnets powered by the same type generator described previously.

There are other advantages of cryogenic operation of electromagnets as exemplified by the Lewis Research Center's system of magnets:

(1) The fields can be swept quite rapidly; and hence, experiments which require fields of this kind are readily accommodated.

(2) Ripple and noise fields are very small, $\approx 10^{-3}$ tesla.

(3) The general design is appropriate for solenoids of still higher field strength - higher than those possible with superconducting magnets made with presently known superconducting materials.

The major disadvantages of cryogenically cooled magnets are (1) the short operating time at maximum field, (2) the large capital investment for the refrigeration plant, (3) the large, bulky, and very heavy magnet coils, and (4) the very large and heavy cryostats needed to ensure enough volume to store the cryogen prior to a run.

Despite these disadvantages the magnets are reliable and produce high-intensity fields for research in basic physics and in engineering applications (refs. 13 to 15).

SUPERCONDUCTIVE MAGNETS

After the development of the high-critical-field superconductors (a conductor made of niobium stannide (Nb_3Sn) was announced in January 1961 by Kunzler, et al., in ref. 16) the Lewis Research Center began a program for the development of high-field, large-volume, superconductive magnets. This program consisted of both in-house and contract research and development. The magnets resulting from this program are described herein.

Magnetic Bottle

A system of coils whose combined field is shown in figure 19 was built as a prototype for plasma physics experiments (refs. 17 to 19). The system consists of two magnetic mirror coils that produce 5 teslas each on the axis of the system and a mirror ratio of 2:1 with the central field. The more uniform central field is provided by inserting a third coil between the two mirror coils, as shown in figure 19. A "minimum B" field which is more effective than the simple mirror field for plasma containment is produced by a sys-

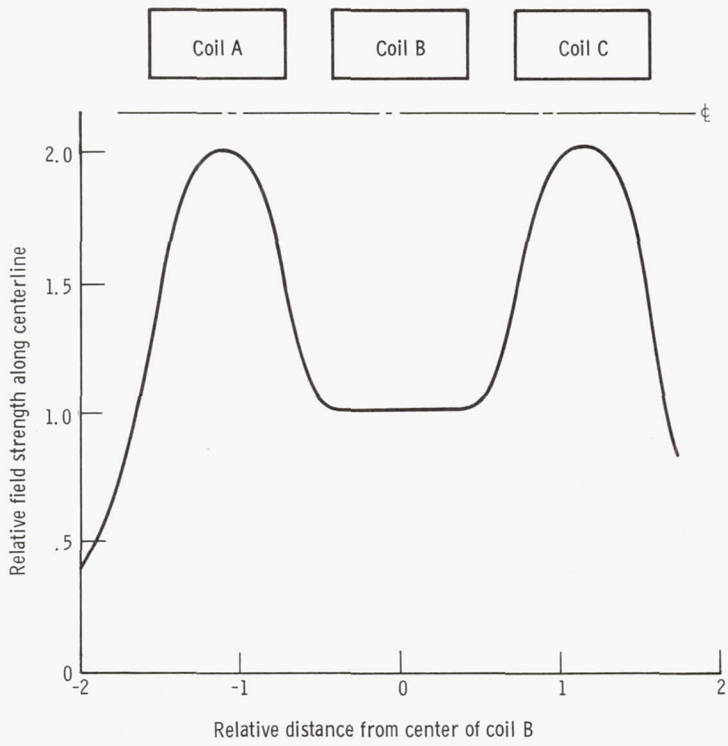

Figure 19. - Magnetic mirror configuration for plasma physics experiments.

tem of linear conductors (Ioffe coils, ref. 20) equally spaced around the inner diameter of the coil forms.

A photograph of the actual quadrupole Ioffe coil is shown in figure 20(a), and the winding scheme is shown in figure 20(b). These Ioffe coils are wound with niobium stannide (copper clad for stability). They operate quite satisfactorily and are not easily driven to the normal state.

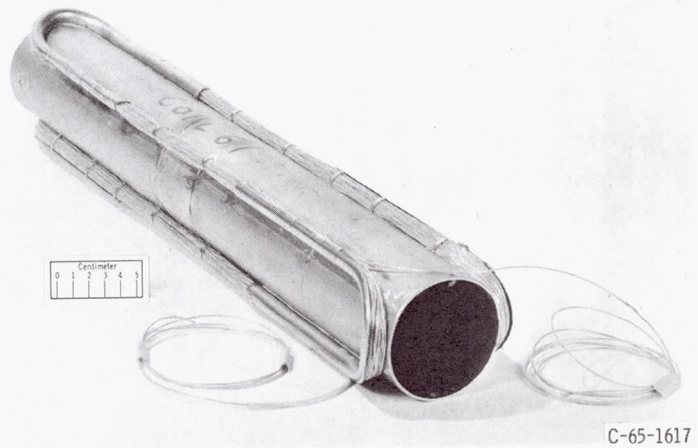

(a) Ioffe coil.

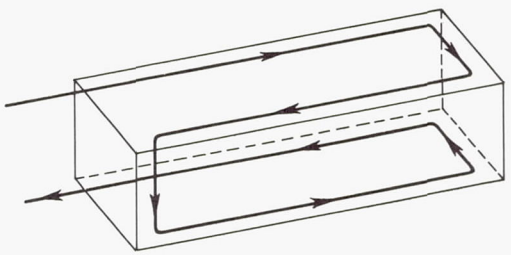

(b) Schematic of current path in coil.

Figure 20. - Ioffe coil (quadrupole configuration).

The three main coils are wound with a seven-strand niobium - 25-atomic-percent-zirconium (Nb-25Zr) cable which is copper plated and dipped in indium. This partially stabilized material is easy to handle and wind into coils. Between turns, insulation is provided by a Mylar film, and aluminum foil provides an energy sink to absorb some of the energy when the coils are driven normal. Monofilament nylon threads (0.05 cm in diam) are wound back and forth between layers of windings to provide passages for the liquid helium to penetrate the windings. The complete magnet is shown in figure 21.

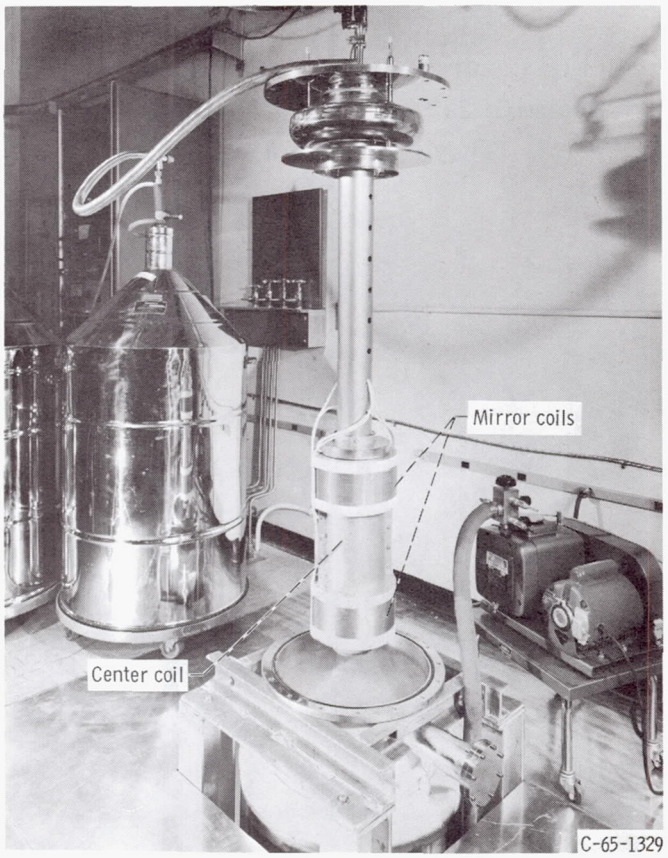

Figure 21. - Magnetic bottle.

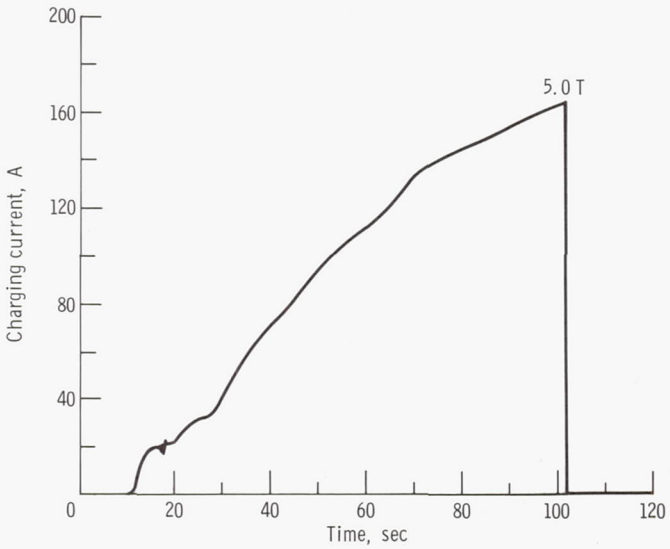

Figure 22. - Charging history of coil A alone.

The performance of the system of coils is best described by showing the variation of coil current as it is increased with time. Figure 22 shows that a mirror coil can be charged in less than 2 minutes and that the design field of 5 teslas is achieved.

Similar coils are being wound with a fully stabilized niobium-titanium conductor in place of the seven-strand niobium-zirconium conductor.

Force-Reduced Toroids

The concept of the force-free magnet has been known and used since the early days in the production of high-field magnets. Pioneers such as Kapitza (ref. 1) and Cockcroft (ref. 21) used the principle of uniform hydrostatic pressure throughout the magnet windings. In more recent times, the concept has been used in various laboratories concerned with the generation of high-intensity fields of large volume for thermonuclear research (refs. 22 and 23).

It can be easily demonstrated, of course, that no finite magnet is truly force-free. Nevertheless, a toroid can be wound so that everywhere the conductor is nearly parallel to the field. In this case, $\vec{j} \times \vec{B}$ (where j is the current, and B is the magnetic field) is small, and there is a reduced normal force on the conductor.

For superconductors, however, there is another advantage of winding the conductor parallel to the local magnetic field. Experiments have shown that superconductors carry more current when placed in longitudinal fields than when placed in transverse fields. Measurements reported in references 24 and 25 show that the critical current is strongly influenced by the angle that the conductor makes with the field. These and other investigations (ref. 26) show that the current can be increased by as much as a factor of 10 or more. In figure 23 the variation of the critical current with the angle θ made by the conductor with the magnetic field is shown for two different superconductors, niobium-zirconium and niobium stannide.

Two force-reduced toroids have been produced for NASA Lewis Research Center under contract. These toroids are wound with niobium - 25-atomic-percent-zirconium wire which has the short-sample critical current-field curves shown in figure 24. The figure shows that the current is at a maximum when the conductor is placed in a 2.5-tesla field parallel to the direction of the current. The NASA toroids were designed to operate in a self-field of this magnitude to take advantage of this increased performance and enhancement factor of about 7. (Dashed lines in fig. 24 indicate this design field.) However, not all this enhancement was realized in the wound coils. The critical currents of the two force-reduced coils were 60 and 63 amperes, respectively (enhanced by a factor of 3 to 4), as compared with 17 to 20 amperes for a conventionally wound coil of the same material.

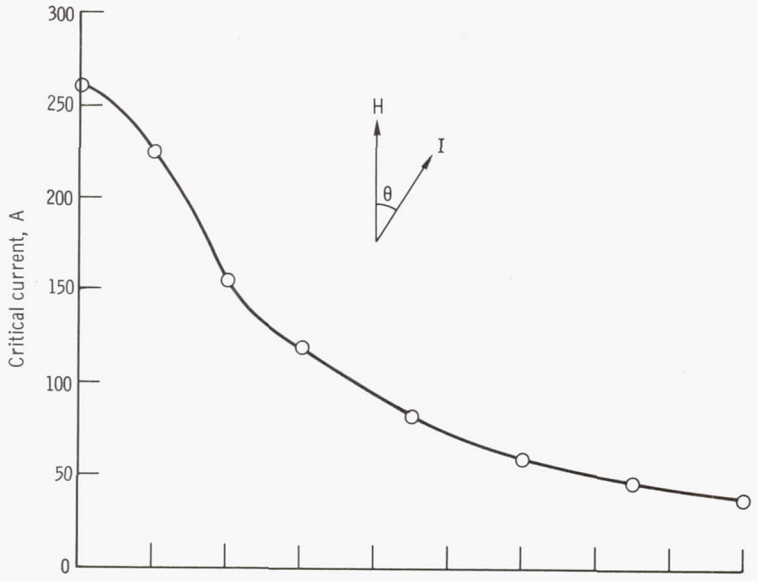

(a) Niobium-zirconium superconductor (ref. 24).

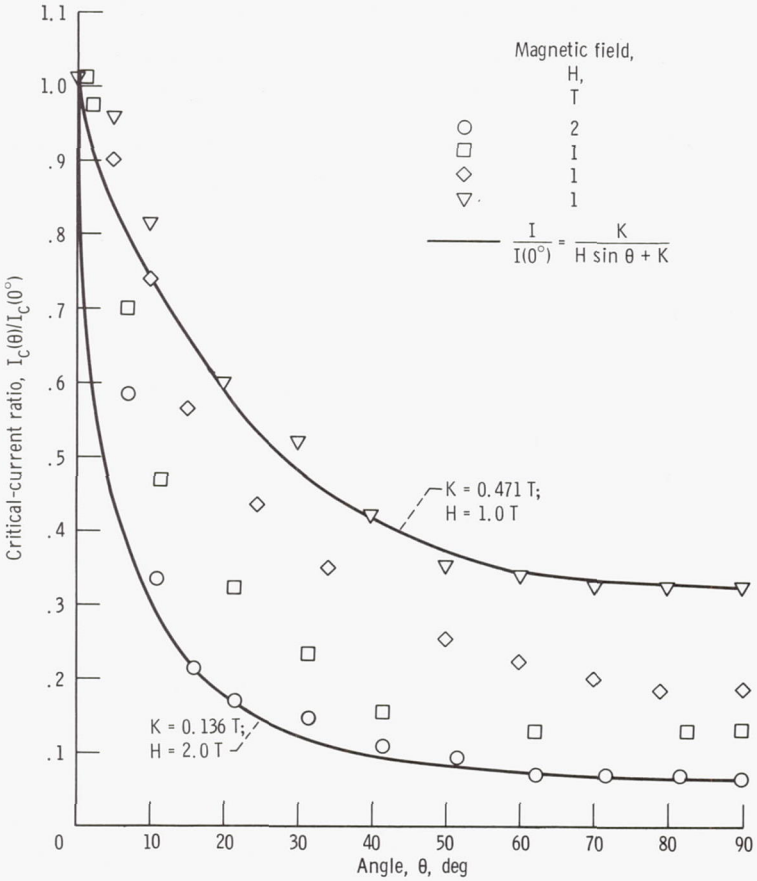

(b) Niobium stannide superconductor (ref. 25).

Figure 23. - Critical current as function of angle made by conductor with magnetic field.

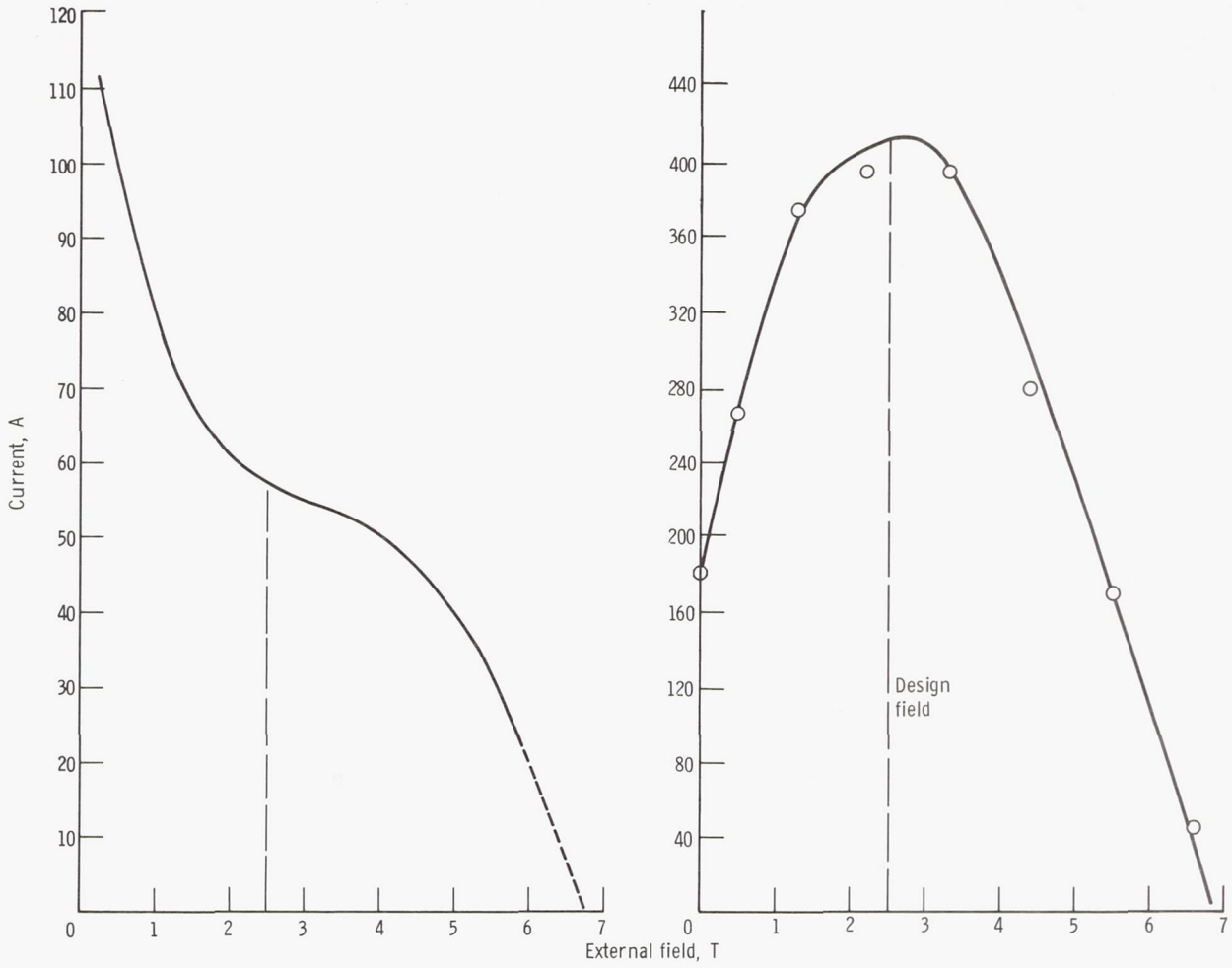

(a) Sample oriented transversely to magnetic field.

(b) Sample oriented parallel to magnetic field.

Figure 24. - Typical curve of short-sample critical current as function of magnetic field for niobium-zirconium wire (ref. 24).

High-Field, Large-Bore Solenoid

To further develop the technology for producing intense, large-volume magnetic fields with superconducting material, it was decided to build a solenoid that would generate a 14-tesla field in a 15-centimeter bore. To produce a field of this magnitude in such a volume by conventional, water-cooled magnets would require many megawatts of power; thus, the advent of high-current, high-field superconductors made such a magnet feasible.

The solenoid was built on contract for the Lewis Research Center (ref. 27). It was wound with a ribbon conductor consisting of niobium stannide vapor deposited on a substrate of stainless steel. At the present, niobium stannide has the highest critical field (>22.0 T) and the highest critical temperature (18.4 K) of any commercially available superconductor. (Recently a superconductor with a critical temperature >20 K was an-

nounced (ref. 28). No details concerning its critical field and critical current are as yet available.) Extensive research during the past several years has failed to find a superconductor that approaches niobium stannide as a useful high-field material. This material can be combined with an exceedingly strong substrate and can be manufactured in a range of sizes to carry a large range of currents. Physical properties of a typical ribbon used in the Lewis 14-tesla magnet are presented in table IV.

The ribbon material is silver plated or copper clad for stabilization of the superconductor and for protection of the superconductor during handling. The ribbon can be wound, unwound, and rewound on a small radius ($\approx$1 cm) without damage to the performance of the superconductor. The short-sample performance is shown in figure 25

TABLE IV. - PHYSICAL PROPERTIES OF NIOBIUM

STANNIDE - STAINLESS STEEL RIBBON (ref. 28)

Property	Stainless steel substrate	Niobium stannide superconductor
Width, cm	0.23	0.23
Thickness, cm	0.008	0.001
Length, km	88	88
Current density, A/cm^2	------	10^6
Tensile strength, N/m^2	16×10^8	16×10^8 (without damage to superconductor)

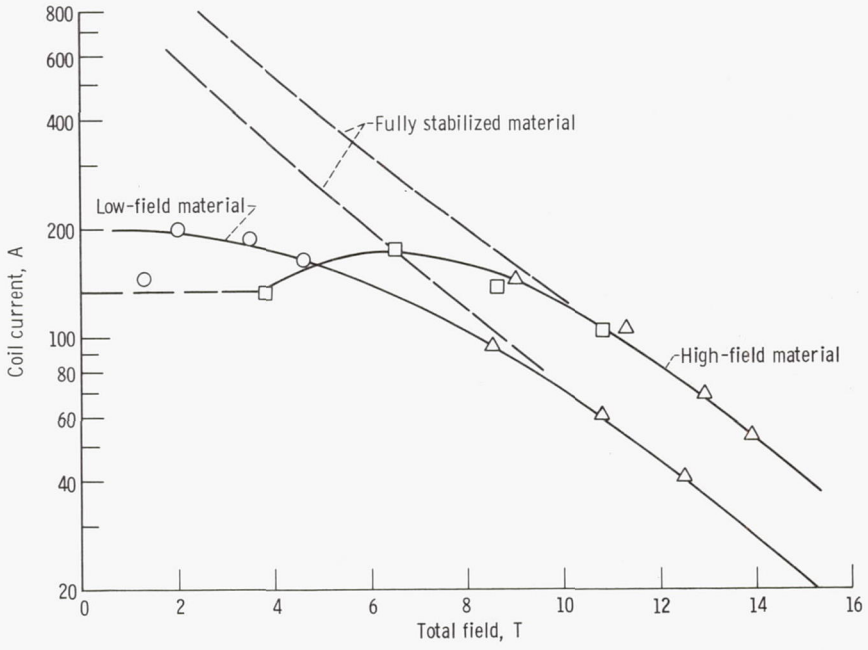

Figure 25. - Critical-current - magnetic-field characteristics of niobium stannide ribbon (ref. 29).

(ref. 29) where the current is plotted as a function of the external field. Also shown are the data for two types of niobium stannide ribbon that were manufactured for specific field ranges.

Since large hoop stresses are encountered in magnet coils of this size (15-cm bore), the effect of stress on the superconductor is an important parameter. Figure 26 shows the effect of stress on copper- and silver-plated niobium stannide ribbon samples that were oriented transversly to the magnetic field with the field parallel to the plane of the ribbon (ref. 30). This transverse relation of current to field occurs at the innermost turns of large solenoids. Figure 26 shows that the critical current density as a function of stress was relatively constant for both types of plating. The critical current density of the copper-plated ribbon increased slightly with stress (fig. 26). Generally, the increase was less than 5 percent. With all the samples, the current density decreased sharply and the sample became resistive just before the breaking point.

The 14-tesla, 15-centimeter-bore solenoid consists of 22 modules, or subcoils, and 20 energy sinks, as shown in figure 27. These modules (one of which is shown being

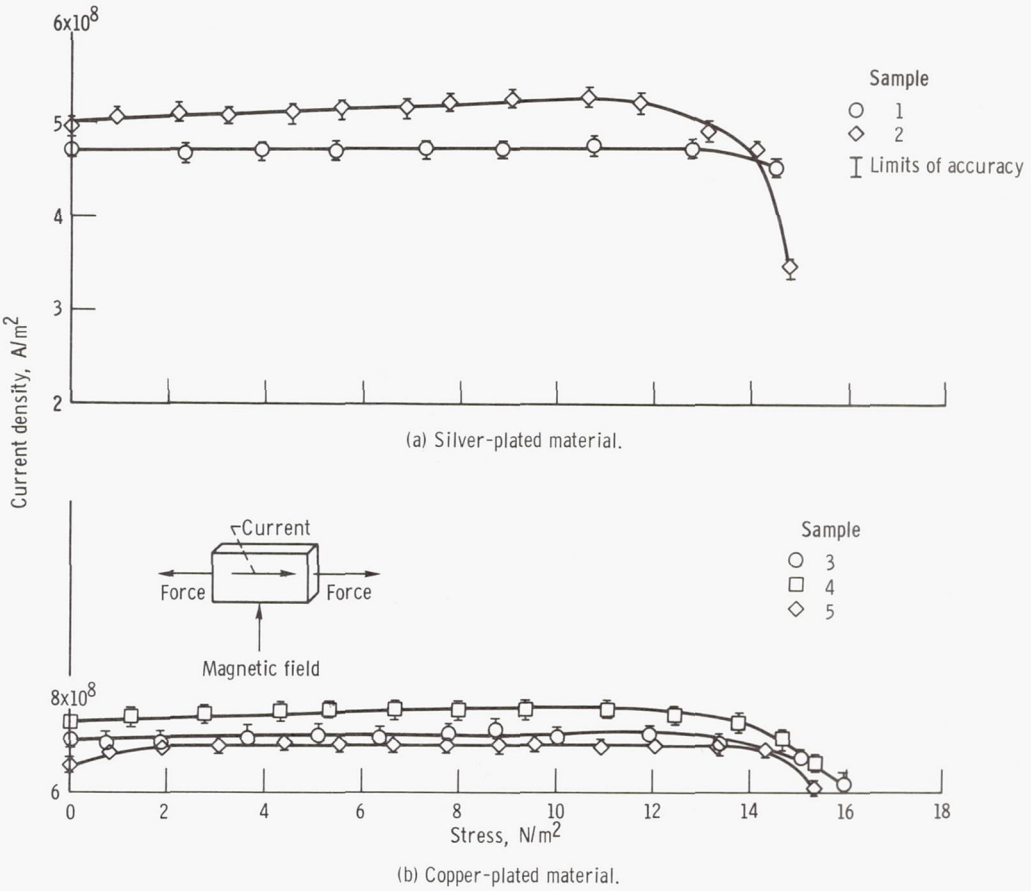

Figure 26. - Effect of stress on current density of niobium stannide ribbon oriented with magnetic field perpendicular to current in plane of ribbon.

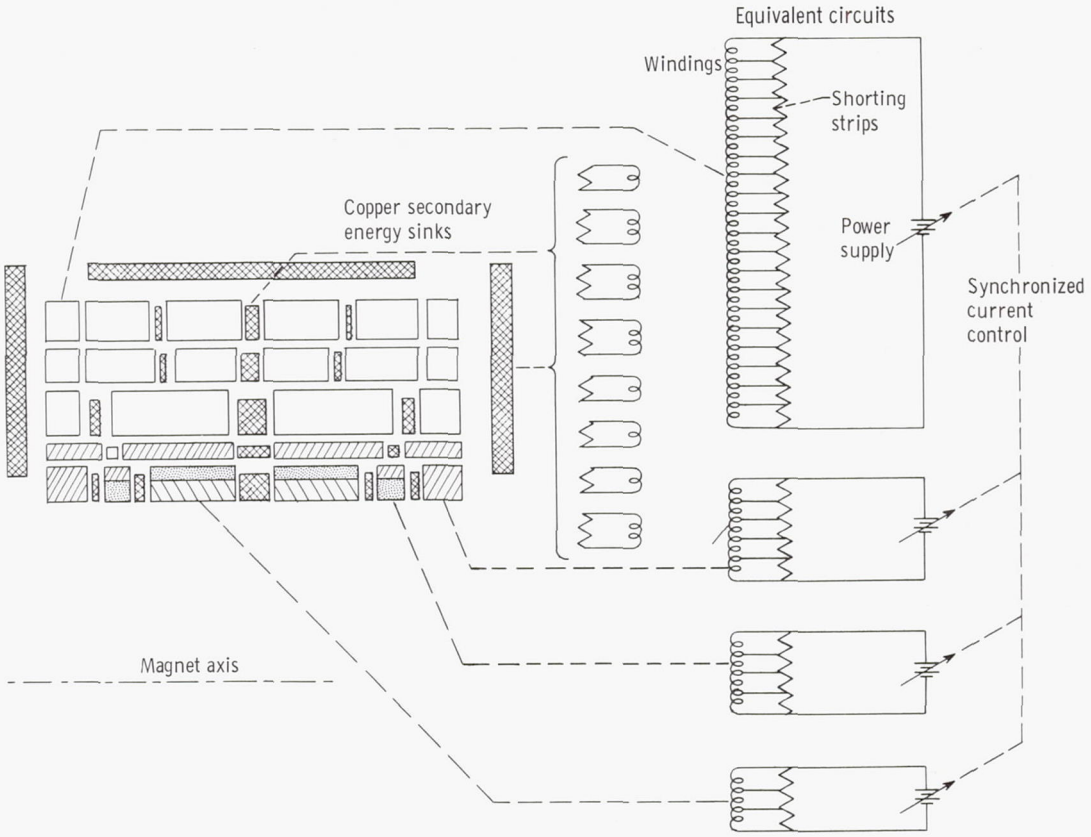

(a) Schematic diagram.

(b) Components.

Figure 27. - High-field, large-bore, superconductive magnet.

Figure 28. - Module of 14-tesla magnet being wound.

wound in fig. 28) were designed to withstand not only the forces which are encountered in their self-field but also the forces developed when the solenoid is placed in external fields in the form of magnetic bottles used for plasma-physics experiments. The energy sinks absorb some of the energy released when the magnet returns to the normal state. The performance of the magnet is shown in figure 29, where the field is plotted as a function of time at different positions in the magnet (ref. 27). The charging time is designed to be 5 to 7 hours, and the current is supplied by four 100-ampere power supplies. Since the time required to cool down and to charge the coils is quite long, it is anticipated that the coils will be kept cold and charged somewhere near capacity at all times.

The control circuitry provides for automatic as well as manual control of the charging and discharging rate. Instrumentation is included within the windings to monitor the magnetic field, the temperature, and the stress on the conductors. The completed magnet is shown in figure 30, and the magnet, Dewar, controls, and instrumentation are shown in figure 31.

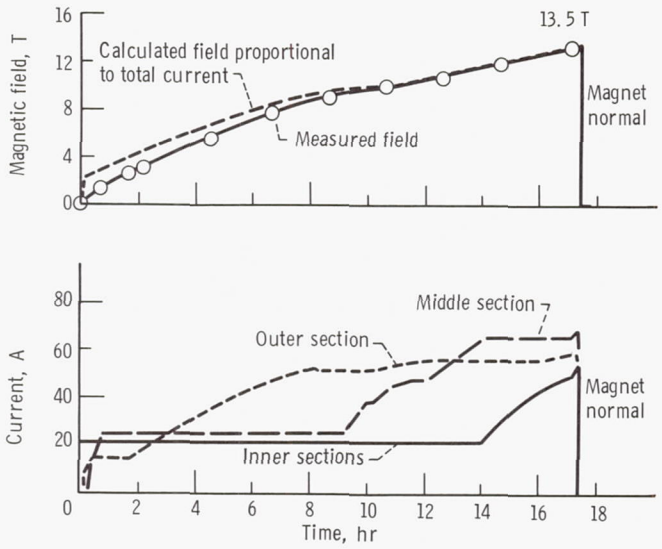

Figure 29. - High-field charging schedule of 15-centimeter-bore magnet.

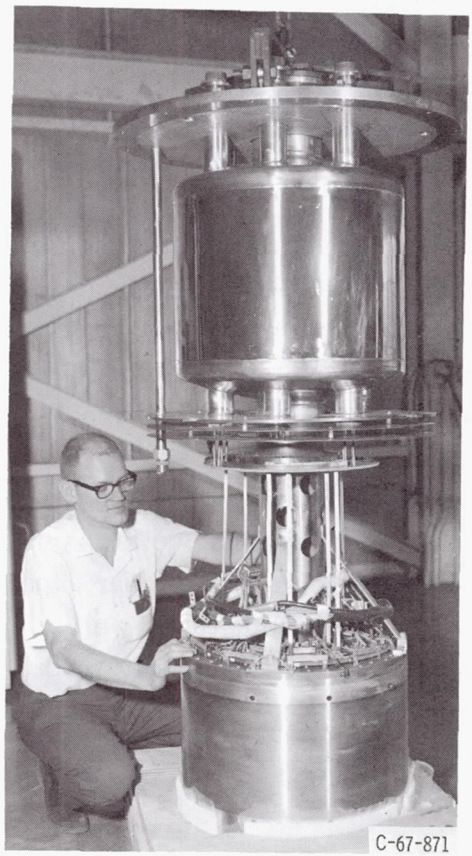

Figure 30. - 15-Centimeter-bore, 14-tesla magnet and Dewar lid.

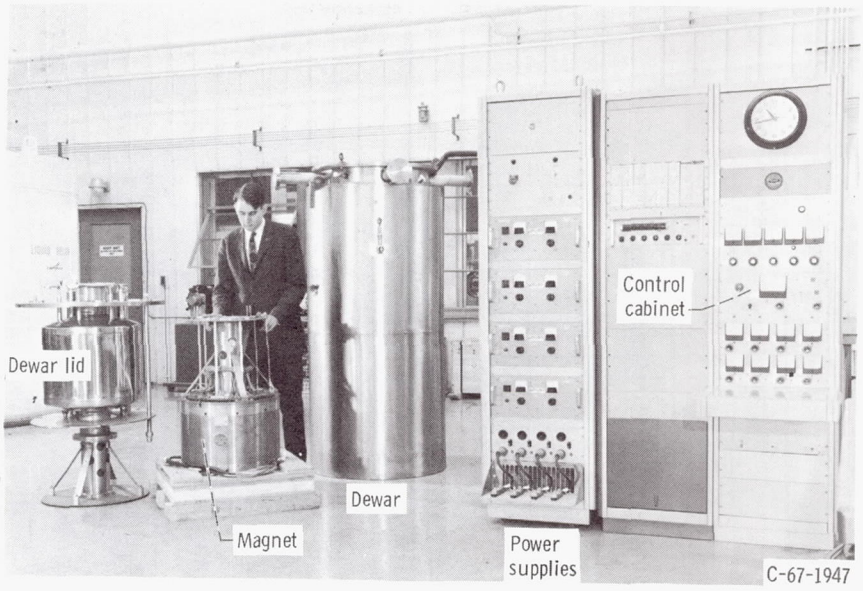

Figure 31. - Magnet system.

Transverse-Field, Iron-Core Solenoid

In 1964 the solid-state physics work at Lewis Research Center generated a need for a magnetic field transverse to the test sample for experiments at liquid-helium temperature.

Adequate field uniformity requires at least a 10-centimeter-diameter bore. Because an attractive force exists between two sets of coils arranged to produce a transverse field, a certain amount of structure is required to support the magnet. It was decided to use an iron-bound configuration to supply the necessary support and a return path for the flux. The magnet shown in figure 32 was designed by Paul R. Aron. Figure 32(a) is a photograph of the magnet and 32(b) is a schematic of the coils and support tube. This configuration had the following advantages: (1) The iron shell would reduce the fringing field, a safety consideration in a crowded laboratory. (2) The field uniformity in the gap would be improved. (3) In the event that the critical current did not prove to be as high as expected, we would be assured of a useful field even at very reduced currents because of the magnetization of the iron.

At the time the design was initiated, copper-clad, 0.025-centimeter-diameter, niobium - 25-atomic-percent-zirconium wire was considered to be the best material; consequently, this material was used in the construction of the magnet. The magnet was wound in the form of pancake coils, 2.5 centimeters in axial thickness. The modular design was chosen to allow replacement of a part of the magnet if damage should occur in

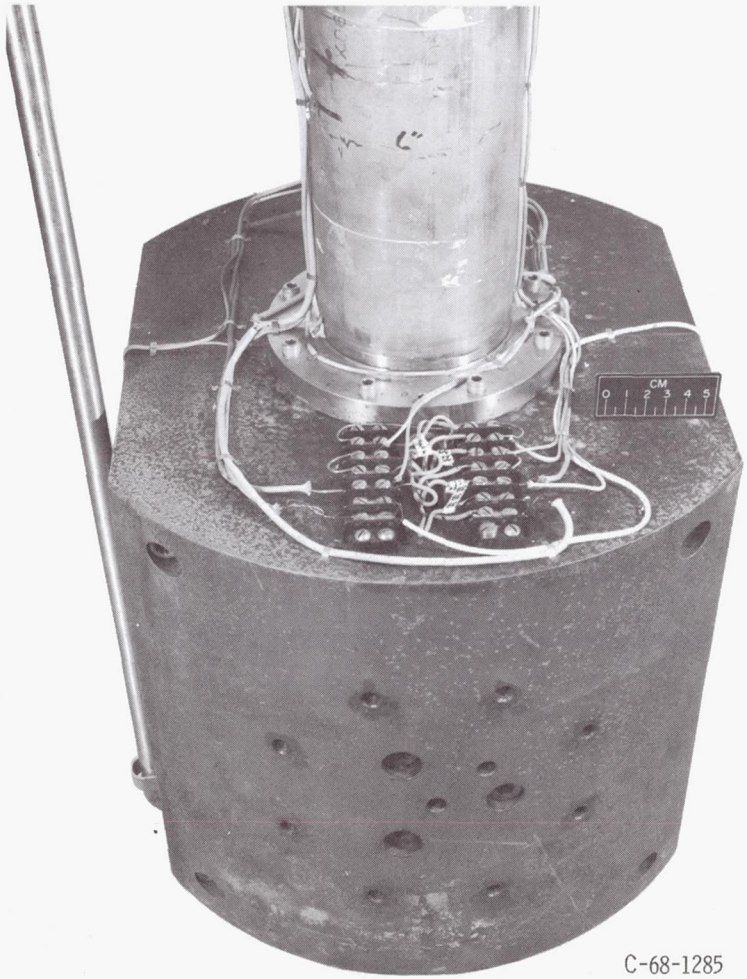

(a) Photograph of magnet.

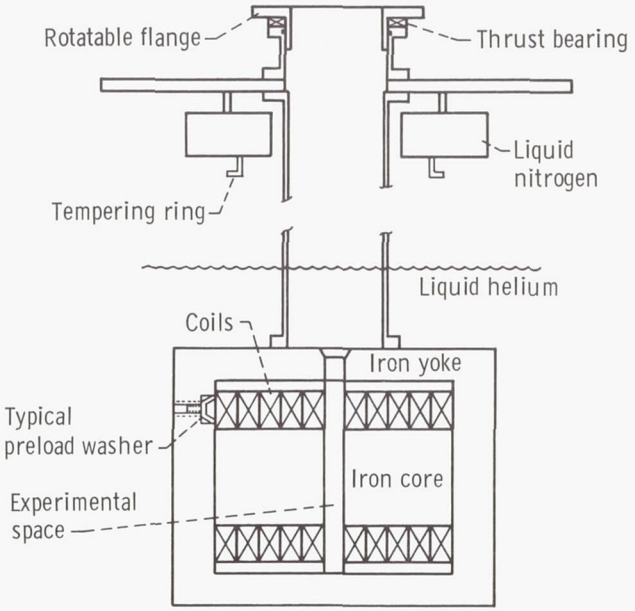

(b) Mechanical schematic of magnet.

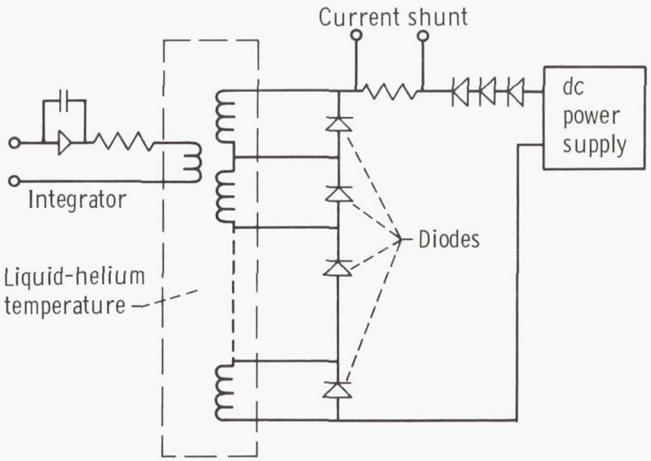

(c) Electrical schematic.

Figure 32. - 11.5-Centimeter-bore, iron-core, superconductive magnet. Transverse field.

service or if the particular batch of wire proved to be degraded in its properties. Also, the modular design would allow useful measurements of the critical current as a function of the number of coils.

There were 10 identical pancakes arranged 5 on each side of the gap. Initial testing showed that the magnet critical current was most predictable if the coils were firmly bolted together; therefore, spring-type washers were used in such a way that a preload was maintained on the coils during cooldown. The coil forms were made of copper to provide a field decay time long enough to prevent damage to the windings during a normalcy. The wire was fully insulated with nylon, and a 0.0025-centimeter-thick Mylar sheet was used between layers and on the inside faces of the coil form flanges. The wire was potted, as it was wound, with an epoxy resin in an attempt to prevent wire movement and to improve the thermal coupling of wire and the bath. Later research has shown, of course, that a better approach is to create open passages to permit the free flow of liquid helium around the wire. The core was machined from iron chosen for its low retentivity and relatively high saturation. The Dewar was designed such that the magnet can be kept in liquid helium over a weekend without attention. This ensures that the magnet can be operable for long periods when the scheduled experimental program is intense. A net saving in money and manpower can result in this mode of operation, since the cost of helium competes with the extra cost in man hours that are required to precool, fill with helium, and then test the magnet before it is ready for operation. The Dewar was also designed such that operation at reduced temperatures is possible, and temperatures down to 1.4 K have been achieved. At the top of the Dewar is a rotatable flange on which the experiment is mounted. This flange is equipped with a motor drive and angular readout. The field is monitored with a fixed coil, in the gap, whose output is integrated. The integrator drift is low enough so that measurements better than 99.9 percent accurate can be made in a period as long as 3 hours.

The magnet is connected electrically in series with reverse diodes across each coil (fig. 32(c)) to prevent the development of high voltages during a normalcy.

The coils were tested individually prior to assembly and exhibited critical currents between 20 and 30 amperes except for two which had critical currents of 7 to 8 amperes. These two coils were not powered in the final assembly and were used only as spacers. Initially the coils were assembled and operated without the iron core and showed sharply degraded critical currents. The maximum critical currents obtained (16 A) were not always reproducible and could be achieved only at impractical low rates of rise. The maximum reliable critical current was 11 amperes. After assembly in the iron yoke, a maximum reliable critical current of 10.7 amperes, producing 3.8 teslas, was achieved at a linear rate of rise of approximately 0.4 tesla per minute. This same rate can be used to drive the magnet down in field.

Achievement of the 10.7-ampere critical current requires 2 to 3 training steps. The

need for this training process, which consumes time and helium, is an added incentive for keeping the magnet superconductive for long periods. The field uniformity was measured perpendicular to the magnet axis and was found to be uniform within ±0.2 percent over 2.5 centimeters at 1.5 teslas and within ±0.7 percent over 2.5 centimeters at 3.5 teslas.

The field on this axis at the midplane is plotted against current in figure 33. The final Dewar boiloff rate with the magnet installed is 0.5 liter per hour and changes very little when the magnet is powered. The magnet has been in service since July 1965 and, when used within the above limits, has proved to be a useful and reliable facility. The vital statistics of this magnet system are summarized in table V. Figure 34 shows a typi-

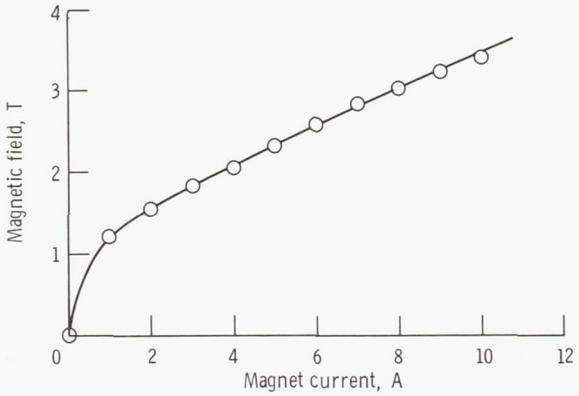

Figure 33. - Magnetic field at center of gap as function of magnet current for iron-core, superconductive magnet.

TABLE V. - SPECIFICATIONS OF 11.5-CENTIMETER-BORE, TRANSVERSE-FIELD, IRON-CORE SUPERCONDUCTIVE MAGNET

Critical current, A	10.7
Maximum field, T	3.8
Gap, cm	2.54
Pole face diameter, cm	11.5
Coil outside diameter, cm	20
Winding diameter, cm	12.8
Yoke material	Ingot iron
Typical number of turns on each module	5700
Length of wire per module, m	2900
Wire material	Nb - 25 at. % Zr
Superconductor diameter, cm	0.0254
Wire plating	Electrolytic copper, 0.0025 cm thick
Wire insulation	Nylon
Maximum rate of change of field, T/min	0.4
Dewar boiloff, liters/day	12
Stored volume of helium, liters	30

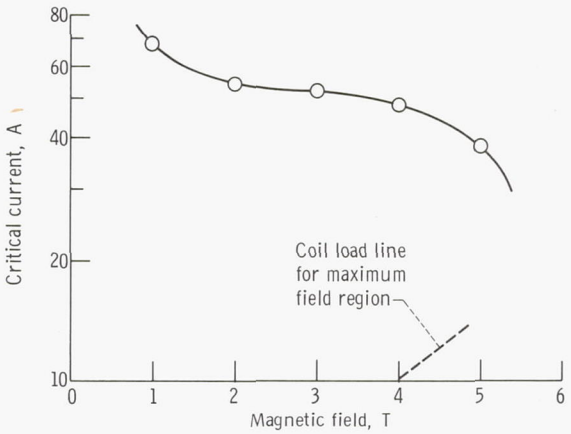

Figure 34. - Short-sample critical current as function of magnetic field for niobium - 25-atomic-percent-zirconium wire. Temperature, 4.2 K.

cal short-sample curve on which the coil load line for the maximum field region is superimposed. The load line (actual operating current-magnetic field relation) shows the relatively low current obtained as compared with the short-sample value.

CONCLUDING REMARKS

Described in this report are several electromagnet systems which have been devel-

TABLE VI. - MAGNET FACILITIES AT NASA LEWIS RESEARCH CENTER

Facility	Coolant	Magnetic field, T	Bore, cm	Length, cm	Power consumed, MW	Operating time
Copper solenoid	Water	11.5	5.0	25	1.52	Continuous
Copper solenoid	Water	9.0	10.0	42	2.07	Continuous
Cryogenically cooled aluminum magnet	Liquid neon	20.0	11.5	50	1.00	[a]1 min
Cryogenically cooled aluminum magnet	Liquid neon	16.0	30.0	75	0	[a]1 min
Superconductive, high-field, large-bore solenoid	Liquid helium	14.0	15.0	29		Continuous
Superconductive magnetic bottle		5.0 (mirror coils), 2.5 (center coil)	10.0	46		
Superconductive, transverse-field, iron-core solenoid		3.0	10.0	NA		
Superconductive, force-reduced toroid		2.5	30.0	NA		

[a]Several runs are possible during a typical day's operation.

oped at Lewis Research Center.

These magnets are water-cooled copper, liquid-neon-cooled aluminum, and superconductive. The highest field strength, 20 teslas in a 11.5-centimeter-diameter cylindrical volume, is produced by the aluminum magnets. The superconductive magnets produce fields as high as 14 teslas in a 15-centimeter-diameter cylindrical volume, while the water-cooled copper magnets produce 10 teslas in a 10-centimeter-diameter cylindrical volume.

The operational characteristics of the magnets described in this report, and summarized in table VI, are adaptable to research in plasma physics, magnetohydrodynamic power generation, solid-state physics, and low-temperature physics.

Lewis Research Center,
National Aeronautics and Space Administration,
Cleveland, Ohio, July 26, 1968,
120-26-09-15-22.

APPENDIX A

HOMOPOLAR GENERATOR CONTROLLER

by Erwin H. Meyn

The controller system (fig. 35) is a closed-loop control. The controller unit generates fixed voltages or variable-slope ramps which terminate at a predetermined fixed voltage (see appendix B). The voltage generated by the controller is an analog of the desired output current from the homopolar generator. Amplifier A-2 compares this voltage with the amplified signal from the shunt which provides a voltage proportional to the output current. The error is amplified by amplifier A-3 and the exciter. This signal drives the output of the homopolar generator through its field to bring the net error to zero and thus bring the output current to the value set by the controller.

The shunt is composed of three 20 000-ampere, 50-millivolt shunts in parallel, which are water cooled for efficient operation up to the generator maximum current of 200 000 amperes.

Manual control is accomplished by connecting the controller output into amplifier A-3 without comparison with the current in amplifier A-2.

The two reversing relays allow for reversal of the exciter field for the purpose of quickly driving the current to zero in an inductive load.

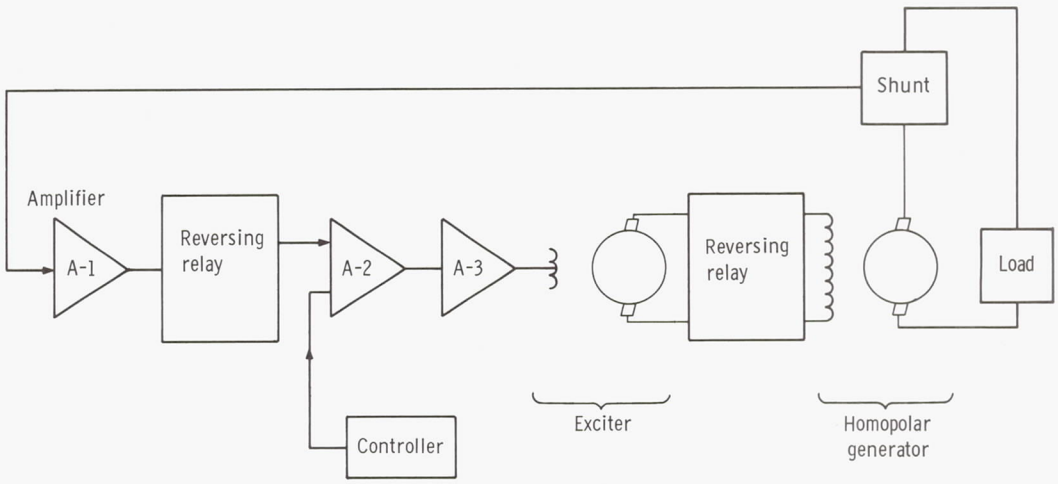

Figure 35. - Control circuit for homopolar generator.

APPENDIX B

ELECTRONIC RAMP-AND-HOLD FUNCTION GENERATOR AS CHARGING CONTROL FOR ELECTROMAGNETS

by Russell J. Jirberg

In the control of many electrical or mechanical systems it is often desirable to operate the system between preset points and to accomplish the change between these points in a linear fashion with time. This mode of control is frequently referred to as the "ramp-and-hold" operation. A typical situation in which this type of control is sought is the energizing of an electromagnet to a preselected magnet field level at a fixed rate so as to maintain a constant charging voltage during the field sweep.

Basically, a voltage ramp function may be generated in a number of ways. Two readily obtained methods utilize (1) the voltage appearing across a capacitor charging from a constant current source, and (2) the voltage at the slidewire of a motor-driven potentiometer fed from a constant voltage source. The first of these methods has been applied to the water-cooled and neon-cooled electromagnets and the second is chosen for the controller of the 14-tesla superconductive magnet described in this report.

The ramp voltage appears at the output of an operational amplifier integrator, the input of which is a constant voltage. The fundamental integrator circuit is shown in figure 36. The ramp is dependent both on the time constant determined by the resistance R and the capacitance C and on the magnitude of the input voltage e_i. Removal of the constant voltage input after a period of integration establishes a "hold" condition.

The complete circuit diagram of the generator is shown in figure 37. The voltage ramp is produced by the operational amplifier 1 (OA-1) stage comprised of the 2-megohm

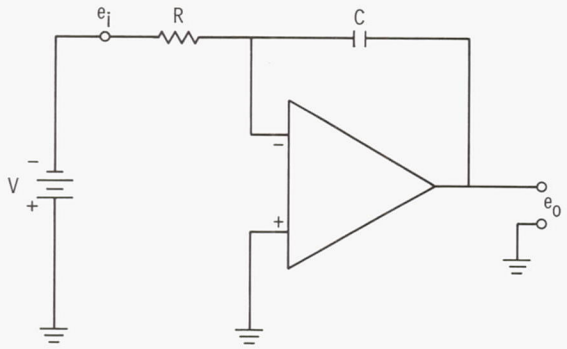

Figure 36. - Integrator circuit.

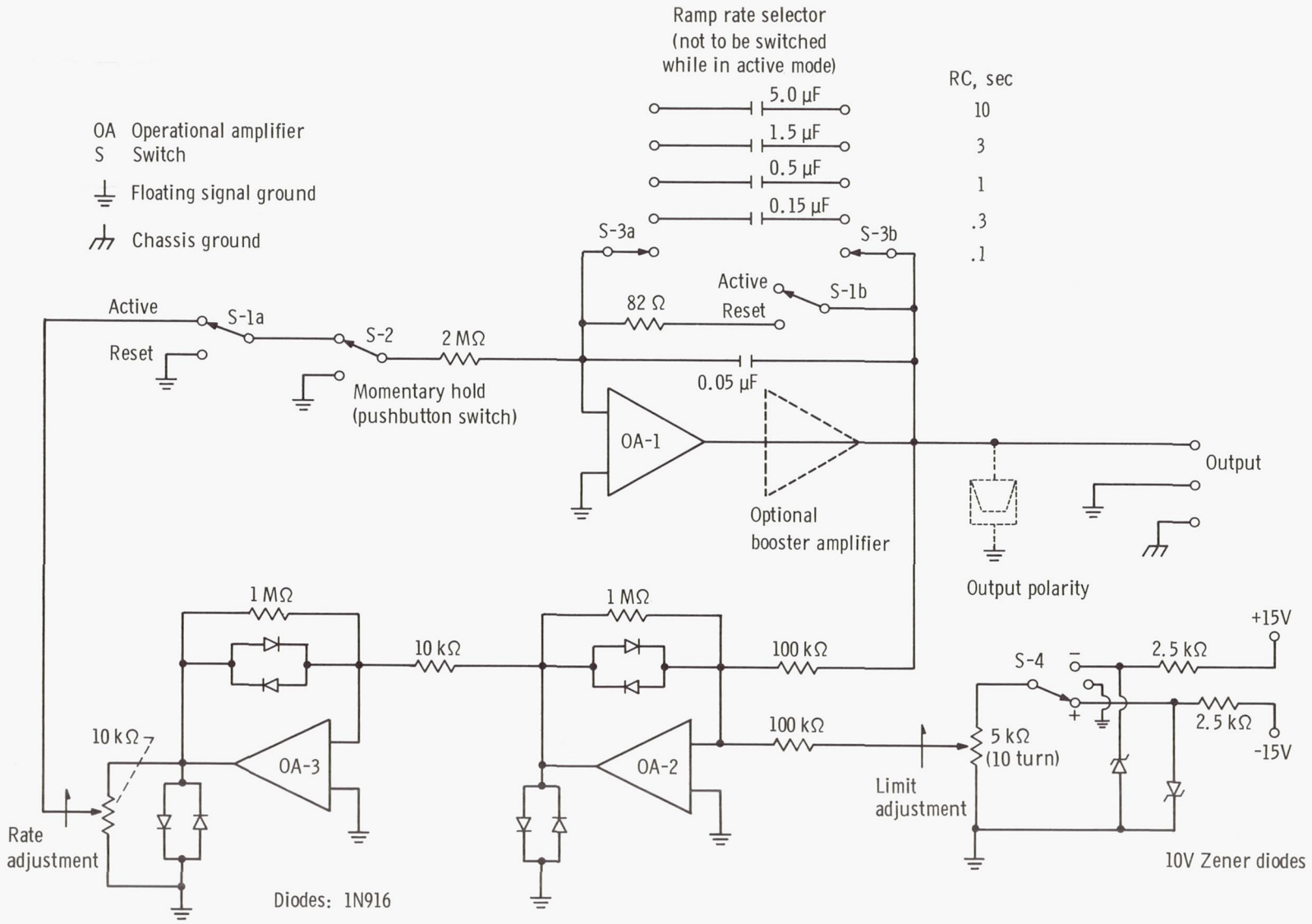

Figure 37. - Electromagnet controller circuit.

input resistor, a series of feedback capacitors so chosen as to permit integrating time constants between 0. 1 and 10 seconds, and a voltage source (the output of OA-3). The OA-3 stage functions as a bipolar switch with a graded null, the characteristics of which are shown in figure 38. During periods when OA-2 drives the input of OA-3 away from zero, the integrator is presented with an essentially constant voltage of approximately 0. 6 volt to integrate and produce the ramp output. When the output of OA-2 is zero the input voltage to the integrator is reduced to zero, and a hold condition results.

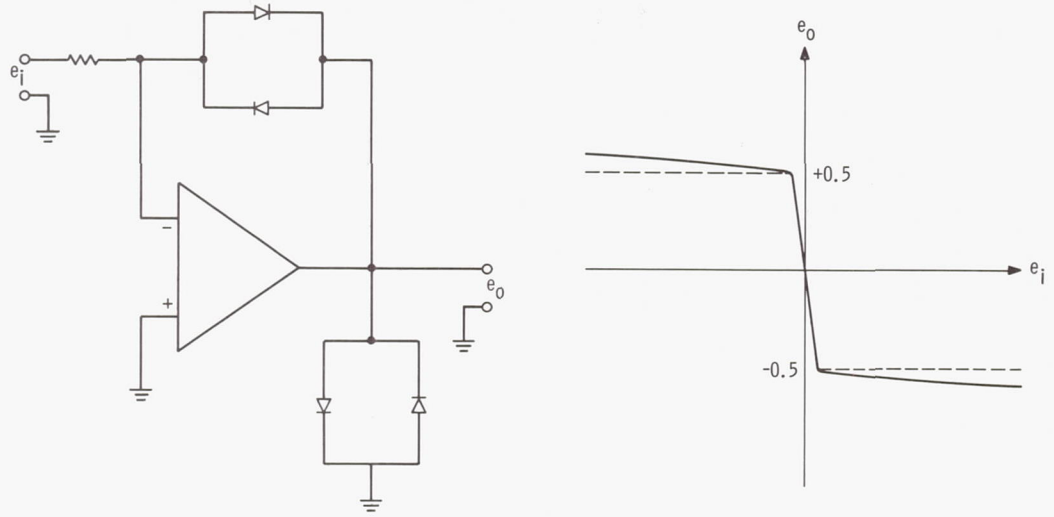

Figure 38. - Characteristics of bipolar switch stage of controller.

The OA-2 stage functions as a voltage comparator which senses the difference in the magnitude of the ramp output to that of the "limit" voltage set by the 10-turn potentiometer. This potentiometer serves as a variable reference and produces an output which switches between nearly constant levels in a manner identical to the action of OA-3. The polarity of the output indicates the sense of the error of the ramp away from the selected limit voltage. Hence, under conditions during which the magnitude of the ramp output is not equal to that of the set limit voltage, a fixed-level voltage appears at the input to the integrator and is phased so as to drive the ramp output to the point set by the "limit" control.

Under this closed-loop mode of control the stability of the hold is determined solely by the stability of the voltage reference. The reference incorporated into the circuit of figure 37 derives its stability from a Zener diode carrying a nearly constant current.

The rate at which the output voltage ramps toward the set point is made adjustable by choice of the integrating time constant (a range adjustment), and by scaling the voltage

presented to the integrator with the potentiometer at the output of OA-3 (a fine adjustment).

The 1-megohm feedback resistors around OA-2 and OA-3 are included to ensure graded nulls and gains not to exceed 10 and 100, respectively. The use of four diode pairs as nonlinear feedback and load elements for OA-2 and OA-3 serves to provide an essentially constant input voltage to the integrator regardless of the magnitude of the error between output and reference.

If it is necessary to interrupt the ramp momentarily during a sweep, a pushbutton (S-2 in fig. 37) is provided to remove the voltage to the integrator and thus produce a hold. This hold condition is, of course, subject to drift; the drift can be minimized by careful adjustment of the offset voltage of OA-1.

Additional controls include a selector switch S-4 for selection of either positive or negative output polarities or the zero potential reference, and a reset switch S-1 to disable the integrator and clamp its output to zero when selecting integrating capacitors or for instantaneous return to zero output.

Before a ramp-and-hold operation, switch S-1 is placed in the "reset" position, switch S-4 is placed in the "0" position, an appropriate time constant is selected with switch S-3, and the limit point is set as indicated on the 10-turn potentiometer. The ramp-and-hold operation is then executed by switching S-1 to "active" and S-4 to either "+" or "-", depending on the desired output polarity.

REFERENCES

1. Kapitza, P.: Method of Obtaining Strong Magnetic Fields. Roy. Soc. Proc., ser. A, vol. 115, Aug. 1927, pp. 658-683.

2. Bitter, F.: The Design of Powerful Electromagnets. Part I. The Use of Iron. Rev. Sci. Inst., vol. 7, no. 12, Dec. 1936, pp. 479-482.

3. Fakan, John C.: The Homopolar Generator as an Electromagnet Power Supply. High Magnetic Fields. Henry Kolm, Benjamin Lax, Francis Bitter and Robert Mills, eds., M.I.T. Press and John Wiley & Sons, Inc., 1962, pp. 211-216.

4. Buchhold, Theodor A.: Cryogenic Flux Pump Switches High Currents. Electronics, vol. 37, no. 12, Mar. 23, 1964, pp. 61-63.

5. Rust, Rudolph; Elleman, D. D.; and Noble, R. M.: JPL Intense Field Air Core Magnet. Tech. Rept. 32-652, Jet Propulsion Lab., California Inst. Tech. (NASA CR-59054), Aug. 31, 1964.

6. Laurence, James C.; Brown, Gerald V.; Geist, Jacob; and Zeitz, Kenneth: A Large Liquid-Neon-Cooled Electromagnet. High Magnetic Fields. Henry Kolm, Benjamin Lax, Francis Bitter and Robert Mills, eds., M.I.T. Press and John Wiley & Sons, Inc., 1962, pp. 170-179.

7. Laurence, James C.; and Coles, Willard D.: Design, Construction, and Performance of Cryogenically Cooled and Superconducting Electromagnets. Proceedings of the International Symposium on Magnet Technology. H. Brechna and H. S. Gordon, eds. AEC Rep. CONF-650922, Oct. 10, 1965, pp. 574-587.

8. Brown, G. V.; and Coles, W. D.: High-Field, Liquid-Neon-Cooled Electromagnets. Advances in Cryogenic Engineering. Vol. 11. K. D. Timmerhaus, ed., Plenum Press, 1966, pp. 638-642.

9. Johnson, Victor J., general ed.: A Compendium of the Properties of Materials at Low Temperature (Phase II). National Bureau of Standards (WADD TR 60-56, pt. 4), Dec. 1961.

10. Hudson, Wayne R.: Copper Magnetoresistance Devices as Magnetometers. NASA TN D-3536, 1966.

11. Geist, J. M.; Kobran, S. Z.; Siegrist, G. W.; and Zeitz, K.: A Helium-Hydrogen Refrigeration System for a Large Liquid-Neon-Cooled Electromagnet. International Advances in Cryogenic Engineering. Vol. 10. K. D. Timmerhaus, ed., Plenum Press, 1965, pp. 46-53.

12. Bewilogua, L.: Neon as a Cooling Agent. Cryogenic Engineering: Present Status and Future Development. Heywood-Temple Industrial Publ., Ltd., London, 1968, p. 38.

13. Hudson, W. R.: Negative Magnetoresistance in Carbon Resistance Thermometers. Rev. Sci. Inst., vol. 39, no. 2, Feb. 1968, pp. 253-254.

14. Woollam, J. A.: Anomalous Shubnikov-De Haas Amplitudes in White Tin. Phys. Letters, vol. 27A, no. 4, July 1, 1968, pp. 246-247.

15. Aron, Paul R.; and Ahlgren, Gary W.: Critical Surfaces for Commercial Nb_3Sn Ribbon and Nb 25% Zr Wire. Presented at the Cryogenic Engineering Conference, Stanford Univ., Stanford, Calif., Aug. 21-23, 1967.

16. Kunzler, J. E.; Buehler, E.; Hsu, F. S. L.; Matthias, B. T.; and Wahl, C.: Production of Magnetic Fields Exceeding 15 Kilogauss by a Superconducting Solenoid. J. Appl. Phys., vol. 32, no. 2, Feb. 1961, pp. 325-326.

17. Coles, Willard D.; Fakan, John C.; and Laurence, James C.: Superconducting Magnetic Bottle for Plasma Physics Experiments. NASA TN D-3595, 1966.

18. Laurence, J. C.; and Coles, W. D.: A Superconducting Magnetic Bottle. Advances in Cryogenic Engineering. Vol. 11. K. D. Timmerhaus, ed., Plenum Press, 1966, pp. 643-651.

19. Laurence, J. C.: Superconductive Magnets at Lewis Research Centre N. A. S. A. Cryogenic Engineering: Present Status and Future Development. Heywood-Temple Industrial Publ., Ltd., London, 1968, pp. 94-98.

20. Gott, Yu. V.; Ioffe, M. S.; and Telkovskii, V. G.: Some New Results on Confinement in Magnetic Traps. Nucl. Fusion, Suppl. 2, pt. 3, 1962, pp. 1045-1047.

21. Cockcroft, J. D.: The Design of Coils for the Production of Strong Magnetic Fields. Phil. Trans. Roy. Soc., vol. 227, 1928, pp. 317-343.

22. Wells, D. R.; and Mills, R. G.: Force-Reduced Toroidal Systems. High Magnetic Fields. Henry Kolm, Benjamin Lax, Francis Bitter and Robert Mills, eds., M. I. T. Press and John Wiley & Sons, Inc., 1962, pp. 44-47.

23. Furth, H. P.; Levine, M. A.; and Waniek, R. W.: Production and Use of High Transient Magnetic Fields. II. Rev. Sci. Inst., vol. 28, no. 11, Nov. 1957, pp. 949-958.

24. Sekula, S. T.; Boom, R. W.; and Bergeron, C. J.: Longitudinal Critical Currents in Cold-Drawn Superconducting Alloys. Appl. Phys. Letters, vol. 2, no. 5, Mar. 1, 1963, pp. 102-104.

25. Cullen, G. W.; Cody, G. D.; and McEvoy, J. P., Jr.: Field and Angular Dependence of Critical Currents in Nb_3Sn. Phys. Rev., vol. 132, no. 2, Oct. 15, 1963, pp. 577-580.

26. Callaghan, Edmund E.: Anisotropic Effects in Helically Wound Solenoids. NASA TN D-2083, 1963.

27. Coles, W. D.; Schrader, E. R.; and Thompson, P. A.: A 14 Tesla 15 cm Bore Superconductive Magnet. Presented at the Cryogenic Engineering Conference, Stanford Univ., Stanford, Calif., Aug. 21-23, 1967.

28. Matthias, B. T.; Geballe, T. H.; Longinotti, L. D.; Corenzwit, E.; Hull, G. W.; Willens, R. H.; and Maita, J. P.: Superconductivity at 20 Degrees Kelvin. Science, vol. 156, no. 3775, May 5, 1967, pp. 645-646.

29. Schrader, E. R.; and Thompson, P. A.: Use of Superconductors with Varied Characteristics for Optimized Design of Large-Bore High-Field Magnets. IEEE Trans. on Magnetics, vol. MAG-2, no. 3, Sept. 1966, pp. 311-315.

30. Hudson, Wayne R.: Effect of Tensile Stress on Current-Carrying Capacity of Commercial Superconductors. NASA TN D-3745, 1966.

NASA-Langley, 1968 —— 23 E-4563

NATIONAL AERONAUTICS AND SPACE ADMINISTRATION
WASHINGTON, D. C. 20546

OFFICIAL BUSINESS

FIRST CLASS MAIL

POSTAGE AND FEES PAID
NATIONAL AERONAUTICS AND
SPACE ADMINISTRATION

POSTMASTER: If Undeliverable (Section 158
Postal Manual) Do Not Retur

"The aeronautical and space activities of the United States shall be conducted so as to contribute . . . to the expansion of human knowledge of phenomena in the atmosphere and space. The Administration shall provide for the widest practicable and appropriate dissemination of information concerning its activities and the results thereof."

—NATIONAL AERONAUTICS AND SPACE ACT OF 1958

NASA SCIENTIFIC AND TECHNICAL PUBLICATIONS

TECHNICAL REPORTS: Scientific and technical information considered important, complete, and a lasting contribution to existing knowledge.

TECHNICAL NOTES: Information less broad in scope but nevertheless of importance as a contribution to existing knowledge.

TECHNICAL MEMORANDUMS: Information receiving limited distribution because of preliminary data, security classification, or other reasons.

CONTRACTOR REPORTS: Scientific and technical information generated under a NASA contract or grant and considered an important contribution to existing knowledge.

TECHNICAL TRANSLATIONS: Information published in a foreign language considered to merit NASA distribution in English.

SPECIAL PUBLICATIONS: Information derived from or of value to NASA activities. Publications include conference proceedings, monographs, data compilations, handbooks, sourcebooks, and special bibliographies.

TECHNOLOGY UTILIZATION PUBLICATIONS: Information on technology used by NASA that may be of particular interest in commercial and other non-aerospace applications. Publications include Tech Briefs, Technology Utilization Reports and Notes, and Technology Surveys.

Details on the availability of these publications may be obtained from:

SCIENTIFIC AND TECHNICAL INFORMATION DIVISION

NATIONAL AERONAUTICS AND SPACE ADMINISTRATION

Washington, D.C. 20546